Inorg. Chem. **1992,** *31,* 5561–5571

Synthesis and Structural Characterization of New Copper Complexes and the Copper–Barium–Alkoxide Complex $BaCu_4(OC(R)C(H)C(R)O)_4(OR')_2(HOR')_4$ ($R = C(CH_3)_3$, $R' = CH_2CH_2OCH_3$)

Wolfgang Bidell, Valery Shklover, and Heinz Berke*

Institute of Inorganic Chemistry, University of Zürich, Winterthurerstrasse 190,
8057 Zürich, Switzerland

Received September 9, 1991

A series of new copper complexes [(thd)Cu(OMe)]$_4$ (**4**), [(tfd)Cu(OMe)]$_4$ (**5**), [(hfd)Cu(OMe)]$_4$ (**6**), [(thd)Cu(OPr^i)]$_2$ (**7**), [(tfd)Cu(OPr^i)]$_2$ (**8**), [(thd)Cu(OPh$_f$)]$_2$ (**9**), [(tfd)Cu(OPh$_f$)]$_2$ (**10**), [(hfd)Cu(OPh$_f$)]$_2$ (**11**), [(thd)Cu(OCH$_2$CH$_2$OMe)]$_4$ (**12**), [(tfd)Cu(OCH$_2$CH$_2$OMe)]$_4$ (**13**), and [(hfd)Cu(OCH$_2$CH$_2$OMe)]$_4$ (**14**) (where thd, tfd, and hfd are the 2,2,6,6-tetramethyl-3,5-heptanedionato-, 1,1,1-trifluoro-2,4-pentanedionato-, and 1,1,1,5,5,5-hexafluoro-2,4-pentanedionato ligands, respectively) were synthesized by using a β-diketonate/alkoxide exchange method. Compounds **6**, **10**, **12**, **14** were characterized by single-crystal X-ray diffraction. **6** and **10** exist as labile THF adducts with four and two THF molecules coordinated to the Cu atoms, respectively. Complex **10** has a centrosymmetric dimeric structure, and complexes **6** and **14** (crystallographic D_2 and C_2 symmetry, respectively) represent a cubane-type tetranuclear structure, in which four expanded parallel Cu···O bonds are observed. Complex **12** (C_i symmetry) also contains a tetranuclear unit but belongs to a group of ladderlike structures with two stronger and two weaker Cu···O contacts. Starting from **12**, the mixed-metal complex **15** was obtained, which was characterized by X-ray single crystal diffractometry. Complex **15** contains one Ba and four Cu atoms and has approximate C_2 symmetry. A unifying approach was applied for the description of the frameworks of **15**, the related Ba, Cu complex **18**, and the high-T_c superconductor **19** in terms of common elementary building blocks. Crystallographic parameters: for **6**, space group *Fddd*, $a = 14.00\ (1)$ Å, $b = 27.75\ (2)$ Å, $c = 29.16\ (1)$ Å, $Z = 8$, $R = 0.0574$, and $R_w = 0.0679$ for 4492 reflections; for **10**, space group $P\bar{1}$, $a = 9.670\ (2)$ Å, $b = 10.054\ (2)$ Å, $c = 10.776\ (3)$ Å, $\alpha = 107.09\ (2)°$, $\beta = 92.15\ (2)°$, $\gamma = 112.07\ (2)°$, $Z = 1$, $R = 0.0532$, and $R_w = 0.0533$ for 2818 reflections; for **12**, space group $P2_1/n$, $a = 12.450\ (5)$ Å, $b = 15.573\ (8)$ Å, $c = 17.324\ (9)$ Å, $\beta = 93.68\ (4)°$, $Z = 2$, $R = 0.0538$, and $R_w = 0.0584$ for 3515 reflections; for **14**, space group $C2/c$, $a = 17.046\ (5)$ Å, $b = 17.211\ (5)$ Å, $c = 17.634\ (3)$ Å, $\beta = 93.50\ (2)°$, $Z = 4$, $R = 0.0599$, and $R_w = 0.0575$ for 2870 reflections; for **15**, space group $P\bar{1}$, $a = 14.285\ (5)$ Å, $b = 16.407\ (5)$ Å, $c = 19.409\ (6)$ Å, $\alpha = 77.57\ (3)°$, $\beta = 89.60\ (3)°$, $\gamma = 81.14\ (3)°$, $Z = 2$, $R = 0.0983$, and $R_w = 0.0983$ for 5579 reflections.

Introduction

The cores of mono- and polynuclear complexes can be structurally related to inorganic materials. Although molecular units are mostly of limited three-dimensional extension, their molecular structure and solid-state packing should reflect some features of similarly composed solids. Of course, the consideration of metal complexes as structural images of extended structure materials may be superficial and should be restricted to the modeling of very local geometrical nearest-neighbor type aspects. Such a kind of analysis was performed with e.g. metal alkoxides, which may serve as models for metal oxides in their structures[1] and in their reactions with a wide variety of chemical agents.[2] A similar model approach[3] was suggested for magnetically dilute and concentrated systems. Polynuclear transition metal complexes form important intermediate cases which allow a rigorous analysis of the interaction between transition metal atoms.

Another challenge for the structural study of certain types of metal complexes is related to their use as chemical precursors in deposition processes of metal oxide materials, e.g. via the chemical vapor or sol–gel techniques.[4] Here structural investigations can assist in the search for certain correlations of practically important factors, e.g. estimates of kinetic pathways from ground-state properties, nonspecific intermolecular interaction,[5] volatility, or thermal stability. The most important properties of inorganic materials are closely connected with "cooperativity" or "communication" of neighboring repeating units[5] and the (X-ray) structural data on even small molecular compounds. The pecularities of preferred intra- or intermolecular contacts and associative phenomena and also the anisotropy of thermal motions or disordering of molecular moieties[6] can give useful information about target inorganic structures.

Experimental Section

General Procedures. All manipulations were performed under an atmosphere of dry nitrogen with use of standard Schlenk techniques. Methanol and 2-methoxyethanol were dried by distillation from Mg fillings, and 2-propanol was dried from CaH_2. Bis(2,2,6,6-tetramethyl-3,5-heptanedionato)copper(II) (Cu(thd)$_2$, **1**), bis(1,1,1-trifluoro-2,4-pentanedionato)copper(II) (Cu(tfd)$_2$, **2**), and bis(1,1,1,5,5,5-hexafluoro-2,4-pentanedionato)copper(II) (Cu(hfd)$_2$, **3**) were prepared by literature methods.[3,7,8] 2,2,6,6-Tetramethyl-3,5-heptanedione (Fluka AG), 1,1,1-trifluoro-2,4-pentanedione (Fluka AG), 1,1,1,5,5,5-hexafluoroacetylacetone (Lancaster), potassium *tert*-butoxide (Fluka AG), pentafluorophenol (Lancaster), and barium granules (<0.8 cm, Alfa) were used without further purification. Melting points were determined by using a Büchi 530 melting point apparatus. No corrections were applied. Infrared spectra were recorded on a FTS 45 Biorad spectrometer as Nujol mulls, with data given in cm^{-1}. Electronic spectra in the visible region (vis) were recorded on a Varian Cary 2300 spectrophotometer. Absorption maxima (λ_{max}) are given in nm with molecular absorption coefficient (ϵ)

---

(1) Bradley, D. C. *Nature* (London) **1958**, *182*, 1211.
(2) Chisholm, M. H. In *Inorganic Chemistry: Towards the 21st Century*. Chisholm, M. H., Ed.; ACS Symp. Ser. **1983**, *211*, 243–290.
(3) Watson, W. H.; Holley, W. W. *Croat. Chem. Acta* **1984**, *57*, 467.
(4) Bradley, D. C. *Chem. Rev.* **1989**, *89*, 1317.
(5) Caulton, K. G.; Hubert-Pfalzgraf, L. G. *Chem. Rev.* **1990**, *90*, 969.
(6) Shklover, V.; Berke, H. *Coord. Chem. Rev.*, in press.
(7) *Beilstein 1* (3), 3123.
(8) Funck, L. L.; Ortolano, T. R. *Inorg. Chem.* **1968**, *7*, 567.

0020-1669/92/1331-5561$03.00/0

in L mol^{-1} cm^{-1} in parentheses, all calculated for dimers, with sh = shoulder. EI mass spectra (MS) (m/e) were recorded on a Finnigan Mat 8320 instrument. Molecular weight determinations (M_r) in g mol^{-1} were obtained with a Knauer vapor pressure osmometer (Type 11.00) at room temperature using chloroform as solvent. Elemental analyses were performed at the Microanalytical Department of the University of Zürich. All compounds mentioned in the next sections are hygroscopic and were therefore stored under nitrogen.

Bis(μ_3-methoxy)bis(μ-methoxy)tetrakis[(2,2,6,6-tetramethyl-3,5-heptanedionato)copper(II)] ([(thd)Cu(OMe)]$_4$) (4). To a suspension of 10.0 g (23.3 mmol) of **1** in 70 mL of methanol was added at room temperature very slowly a solution of 2.6 g (23.3 mmol) of potassium *tert*-butoxide in 15 mL of warm methanol. The color of the suspension changed immediately from violet to blue. After 2 h a blue precipitate was filtered off, washed three times with 30 mL of cold MeOH, and dried in vacuo: yield 95%; mp 222–224 °C; dec >235 °C; subl 120 °C, 10^{-4} Torr. Anal. Calcd for $C_{48}H_{88}O_{12}Cu_4$: C, 51.87; H, 7.98; Cu, 22.87. Found: C, 51.65; H, 7.84; Cu, 22.71. Vis: THF, 587 (110); $CHCl_3$, 653 (82), 583 (77). M_r: found, 676 (calcd for $[(thd)Cu(OMe)]_n$, 555 (n = 2) and 1111 (n = 4)). MS: 556 ($[M]^+/2$, $^{63}Cu/^{65}Cu$), 525 ($[M]^+/2 - (OCH_3)$), 494 ($[M]^+/2 - 2(OCH_3)$), ($[M]^+/2 - 2(OCH_3) - Cu$, ^{65}Cu). IR: 1568 (vs, $\nu_{(C=O)}$), 1553 (s, $\nu_{(C=O)}$), 1536 (s), 1504 (s), 1387 (s), 1360 (s), 1246 (w), 1223 (m), 117 (w), 1148 (m), 1078 (w), $\nu_{(C-O)(\mu\text{-}OMe)}$), 1046 (m, $\nu_{(C-O)(\mu\text{-}OMe)}$).

Tetrakis(μ_3-methoxy)tetrakis[(1,1,1-trifluoro-2,4-pentanedionato)copper(II)] ([(tfd)Cu(OMe)])$_4$ (5). **5** was prepared as above, starting from **2**: Turquoise blue solid; yield 97%; mp 204–208 °C (dec); subl 115 °C, 10^{-1} Torr. Anal. Calcd for $C_{24}H_{28}F_{12}O_{12}Cu_4$: C, 29.10; H, 2.85; F, 23.02; Cu, 25.66. Found: C, 29.36; H, 2.91; F, 22.64; Cu, 24.73. Vis: THF, 636 (90); $CHCl_3$, 650 (98). M_r: found, 668 (calcd for $[(tfd)Cu(OMe)]_n$, 495 (n = 2) and 991 (n = 4)). MS: 496 ($[M]^+/2$, $^{63}Cu/^{65}Cu$), 465 ($[M]^+/2 - (OCH_3)$), 434 ($[M]^+/2 - 2(OCH_3)$), 371 ($[M]^+/2 - 2(OCH_3) - Cu$, ^{65}Cu). IR: 1623 (vs, $\nu_{(C=O)}$), 1607 (s), 1527 (m), 1302 (s), 1226 (m), 1191 (m), 1138 (s), 1034 (m, $\nu_{(C-O)(\mu\text{-}OMe)}$).

Tetrakis(μ_3-methoxy)tetrakis[(1,1,1,5,5,5-hexafluoro-2,4-pentanedionato)copper(II)] ([(hfd)Cu(OMe)]$_4$) (6). **6** was prepared as described for **4**, starting from **3**, except that less methanol was used, because of the good solubility of **6** therein: Dark green solid; yield 45%; mp 252–254 °C (dec); subl 100 °C, 10^{-1} Torr. Single crystals of **6**·4THF suitable for X-ray diffraction were obtained from recrystallization from 5:1 hexane/THF. They lose THF upon drying in vacuo. Anal. Calcd for $C_{24}H_{16}F_{24}O_{12}Cu_4$: C, 23.89; H, 1.34; F, 37.79; Cu, 21.07. Found: C, 24.42; H, 1.72; F, 37.40; Cu, 21.20. Vis: THF, 673 (99); $CHCl_3$, 685 (183). MS: 603 ($[M]^+/2$, $^{63}Cu/^{65}Cu$), 572 ($[M]^+/2 - (OCH_3)$), 541 ($[M]^+/2 - 2(OCH_3)$), 478 ($[M]^+/2 - 2(OCH_3) - Cu$, ^{65}Cu). IR: 1646 (vs, $\nu_{(C=O)}$), 1607 (w), 1560 (m), 1530 (m), 1475 (s), 11259 (vs), 1199 (s), 1147 (s), 1113 (m), 1018 (m, $\nu_{(C-O)(\mu\text{-}OMe)}$).

Bis(μ-isopropoxy)bis[(2,2,6,6-tetramethyl-3,5-heptanedionato)copper(II)] ([(thd)Cu(OPr^i)]$_2$) (7). **7** was prepared as described for **4**, except that 2-propanol was used instead of methanol: Olive blue solid; yield 91%; mp 198–202 °C (dec); subl 140 °C, 10^{-1} Torr. Anal. Calcd for $C_{28}H_{52}O_6Cu_2$: C, 54.98; H, 8.51; Cu, 20.80. Found: C, 54.81; H, 8.57; Cu, 20.33. Vis: THF, 585 (146); $CHCl_3$, 603 (118), 515 (120). M_r: found 650 (calcd for $[(thd)Cu(OPr^i)]_2$, 661). MS: no $[M]^+$ peak observed, only 494 ($[M]^+ - 2(OPr^i)$, $^{63}Cu/^{65}Cu$), 431 ($[M]^+ - 2(OPr^i) - Cu$, ^{65}Cu). IR: 1568 (vs, $\nu_{(C=O)}$), 1555 ($\nu_{(C=O)}$), 1539 (s), 1506 (s), 1389 (s), 1360 (s), 1246 (w), 1224 (m), 1179 (w), 1149 (m), 1139 (m).

Bis(μ-isopropoxy)bis[(1,1,1-trifluoro-2,4-pentanedionato)copper(II)] ([(tfd)Cu(OPr^i)]$_2$) (8). **8** was prepared as for **4** using **2** as the starting compound and 2-propanol as the solvent: Dark green solid; yield 65%; mp 209–211 °C (dec); subl 110 °C, 5×10^{-2} Torr. Anal. Calcd for $C_{16}H_{22}O_6F_6Cu_2$: C, 34.85; H, 4.02; F, 20.67; Cu, 23.05. Found: C, 34.84; H, 4.23; F, 20.43; Cu, 23.06. Vis: THF, 625 (104); $CHCl_3$, 650 (99). M_r: found, 720 (calcd for $[(tfd)Cu(OPr^i)]_n$, 551 (n = 2) and 1103 (n = 4)). MS: no $[M]^+$ peak was observed, only 434 ($[M]^+ - 2(OPr^i)$, $^{63}Cu/^{65}Cu$), 371 ($[M]^+ - 2(OPr^i) - Cu$, ^{65}Cu). IR: 1619 (vs, $\nu_{(C=O)}$), 1617 (vs), 1529 (m), 1303 (s), 1227 (m), 1195 (m), 1140 (s).

Bis(μ-((pentafluorophenyl)oxy))bis[(2,2,6,6-tetramethyl-3,5-heptanedionato)copper(II)] ([(thd)Cu(OPh$_f$)]$_2$) (9). To a solution of 2.0 g (3.3 mmol) of **7** in 50 mL of THF at room temperature was added 1.2 g (6.6 mmol) of pentafluorophenol. After 1 h the moss green solution was concentrated to 10 mL and 50 mL of hexane was added. The olive green microcrystalline solid that formed was filtered off and dried in vacuo. The filtrate was allowed to stand 2 d at –30 °C, producing an additional crop of green crystals of **9** that were isolated and dried in vacuo: total yield 85%; mp 298–302 °C; subl 170 °C, 10^{-1} Torr. Compound **9** is slightly soluble in hexane and toluene, soluble in ether, and very soluble in THF, $CHCl_3$, and CH_2Cl_2. Anal. Calcd for $C_{34}H_{38}F_{10}O_6Cu_2$: C, 47.50; H, 4.46; F, 22.09; Cu, 14.78. Found: C, 47.43; H, 4.19; F, 21.84; Cu, 14.16. Vis: THF, 690 (163); $CHCl_3$, 540 (147), 634 (sh, 128). M_r: found, 1169 (calcd for $[(thd)Cu(OPh_f)]_n$, 860 (n = 2) and 1720 (n = 4)). MS: 860 ($[M]^+$, $^{63}Cu/^{65}Cu$), 676 ($[M]^+ - (OPh_f)$), 494 ($[M]^+ - 2(OPh_f)$), 431 ($[M]^+ - 2(OPh_f) - Cu$, ^{65}Cu). IR: 1567 (m, $\nu_{(C=O)}$), 1554 (s, $\nu_{(C=O)}$), 1538 (m), 1511 (vs), 1380 (s), 1359 (m), 1246 (w), 1223 (m), 1180 (w), 1146 (m), 1016 (m), 1000 (s), 986 (s).

Bis(μ-((pentafluorophenyl)oxy))bis[(1,1,1-trifluoro-2,4-pentanedionato)copper(II)] ([(tfd)Cu(OPh$_f$)]$_2$) (10). Upon slow addition of 1.4 g (7.3 mmol) of pentafluorophenol to a solution of 2.0 g (1.8 mmol) of **8** in 25 mL THF, the color changed from dark green to moss green. Stirring at room temperature was continued for 1 h, and the reaction mixture was evaporated to dryness. The resulting green powder was washed two times with 15 mL of hexane and dried in vacuo: yield 90%; mp 193–196 °C; dec >240 °C; subl 110 °C, 10^{-1} Torr. Recrystallization from 10:1 hexane/THF at –30 °C produced dark green crystals of **10**·2THF suitable for X-ray diffraction, but they lose solvated THF upon drying. Product **10** is very slightly soluble in hexane and toluene, slightly soluble in ether, and very soluble in THF, $CHCl_3$, and CH_2Cl_2. Anal. Calcd for $C_{22}H_8O_6F_{16}Cu_2$: C, 33.06; H, 1.01; F, 38.03; Cu, 15.90. Found: C, 33.26; H, 1.23; F, 37.79; Cu, 15.86. Vis: THF, 743 (153); $CHCl_3$ 615 (113), 555 (114). M_r: found, 910 (calcd for $[(tfd)Cu(OPh_f)]_n$, 799 (n = 2) and 1599 (n = 4)). MS: 800 ($[M]^+$, $^{63}Cu/^{65}Cu$), 617 ($[M]^+ - (OPh_f)$), 434 ($[M]^+ - 2(OPh_f)$), 371 ($[M]^+ - 2(OPh_f) - Cu$, ^{65}Cu). IR: 1619 (s, $\nu_{(C=O)}$), 1601 (m), 1535 (m), 1516 (vs), 1311 (s), 1305 (s), 1231 (m), 1197 (m), 1150 (s), 1144 (s), 1019 (s), 995 (vs), 954 (m).

Bis(μ-((pentafluorophenyl)oxy))bis[(1,1,1,5,5,5-hexafluoro-2,4-pentanedionato)copper(II)] ([(hfd)Cu(OPh$_f$)]$_2$) (11). A solution of 2.0 g (1.7 mmol) of **6** in 50 mL of THF was treated with 1.2 g (6.6 mmol) of pentafluorophenol. After 1 h the resulting brown green solution was evaporated to dryness. The crude product was recrystallized from 5:1 hexane/ether at –80 °C. The resulting green crystals were collected by filtration and dried in vacuo: yield 75%; mp 117–121 °C; dec >255 °C; subl 95 °C, 10^{-1} Torr. Compound **11** is soluble in hexane and very soluble in ether, THF, $CHCl_3$, and CH_2Cl_2. Anal. Calcd for $C_{22}H_2O_6F_{22}Cu_2$: Cu, 14.01. Found: Cu, 13.64. Vis: THF, 785 (103); $CHCl_3$, 670 (205). M_r: found, 1064 (calcd for $[(hfd)Cu(OPh_f)]_n$, 907 (n = 2) and 1815 (n = 4)). MS: 907 ($[M]^+$, $^{63}Cu/^{65}Cu$), 724 ($[M]^+ - (OPh_f)$), 541 ($[M]^+ - 2(OPh_f)$), 478 ($[M]^+ - 2(OPh_f) - Cu$, ^{65}Cu). IR: 1650 (s, $\nu_{(C=O)}$), 1616 (w), 1561 (w), 1511 (vs), 1257 (s), 1212 (s), 1158 (s), 1147 (s), 1111 (m), 1046 (w), 1016 (m), 996 (s).

Bis(μ_3-(2-methoxyethoxy))bis(μ-(2-methoxyethoxy))tetrakis[(2,2,6,6-tetramethyl-3,5-heptanedionato)copper(II)] ([(thd)Cu(OCH$_2$CH$_2$OMe)]$_4$) (12). To a mixture of 50 mL of 2-methoxyethanol and 10 mL of THF was added 10.0 g (16.4 mmol) of **7**. The resulting dark blue suspension was heated for 2 h at 50 °C, after which stirring was continued at room temperature overnight. A dark blue solid was collected by filtration and dried in vacuo. The remaining filtrate was left for 2 d at –30 °C, and an additional crop of crystals were obtained and dried in vacuo: total yield 75%; mp 91–93 °C; dec >229 °C; subl 90 °C, 10^{-1} Torr. **12** is slightly soluble in ether, hexane, and 2-methoxyethanol and soluble in THF, CH_2Cl_2, and $CHCl_3$. Anal. Calcd for $C_{28}H_{52}O_8Cu_2$: C, 52.24; H, 8.14; Cu, 19.74. Found: C, 52.00; H, 8.03; Cu, 19.62. Vis: THF, 605 (103), 560 (sh, 95); $CHCl_3$, 603 (90), 503 (84). M_r: found, 721 (calcd for $[(thd)Cu(OCH_2CH_2OMe)]_n$, 644 ($n$ = 2) and 1288 (n = 4)). MS: 707 ($[M]^+/2 + Cu$, $^{63}Cu/^{63}Cu/^{65}Cu$), 644 ($[M]^+/2$, $^{63}Cu/^{65}Cu$), 613 ($[M]^+/2 - (OMe)$), 569 ($[M]^+/2 - (OCH_2CH_2OMe)$), 494 ($[M]^+/2 - 2(OCH_2CH_2OMe)$), 461 ($[M]^+/2 - (thd)$), 431 ($[M]^+/2 - 2(OCH_2CH_2OMe) - Cu$, ^{65}Cu), 386 ($[M]^+/2 - (OCH_2CH_2OMe) - (thd)$, $^{63}Cu/^{65}Cu$). IR: 1568 (vs, $\nu_{(C=O)}$), 1553 (s, $\nu_{(C=O)}$), 1536 (m), 1503 (s), 1396 (s), 1389 (s), 1360 (m), 1246 (w), 1224 (m), 1181 (m), 1147 (m), 1125 (m), 1088 (m).

Tetrakis[μ_3-(methoxyethoxy)]tetrakis[(1,1,1-trifluoro-2,4-pentanedionato)copper(II)] ([(tfd)Cu(OCH$_2$CH$_2$OMe)]$_4$ (13). To a rapidly stirred suspension of 10.0 g (27.0 mmol) of **2** in 20 mL of 2-methoxyethanol was added at room temperature dropwise 3.03 g (27.0 mmol) of potassium *tert*-butoxide in 15 mL of 2-methoxyethanol. The resulting deep green suspension was stirred for 4 h. The green solid was collected by filtration, washed three times with 7 mL of 2-methoxyethanol, and dried in vacuo: yield 70%; mp 103–106 °C; dec >170 °C; subl 125 °C, 10^{-1} Torr. **13** is soluble in hexane, 2-methoxyethanol, and ether and very soluble in THF, $CHCl_3$, and CH_2Cl_2. Anal. Calcd for $C_{16}H_{22}F_6O_8Cu_2$: C, 32.94; H, 3.80; F, 19.54; Cu, 21.78. Found: C, 33.26; H, 3.86; F, 19.31; Cu, 20.34. Vis: THF, 640 (90); $CHCl_3$, 650 (96). M_r: found, 830 (calcd

Table I. Crystallographic Data for Compounds **6**, **10**, **12**, **14**, and **15**

	compd				
	6	**10**	**12**	**14**	**15**
formula	$C_{24}H_{16}F_{24}O_{12}Cu_4$	$C_{22}H_8O_6F_{16}Cu_2$	$C_{56}H_{104}O_{16}Cu_4$	$C_{32}H_{32}F_{24}O_{16}Cu_4$	$C_{62}H_{118}O_{20}BaCu_4$
M_r	1206.6	799.4	643.9	1188.8	1575.3
a (Å)	14.00 (1)	9.670 (2)	12.450 (5)	17.046 (5)	14.285 (5)
b (Å)	27.75 (2)	10.054 (2)	15.573 (8)	17.211 (5)	16.407 (5)
c (Å)	29.16 (1)	10.776 (3)	17.324 (9)	17.634 (3)	19.409 (6)
α (deg)	90	107.09 (2)	90	90	77.57 (3)
β (deg)	90	92.15 (2)	93.68 (4)	93.50 (2)	89.60 (3)
γ (deg)	90	112.07 (2)	90	90	81.14 (3)
V (Å^3)	11330 (13)	915.0 (3)	3352 (3)	5164 (2)	4388 (2)
d_{calc} (g·cm^{-3})	1.762	1.722	1.283	1.789	1.200
Z	8	1	2	4	2
space group	$Fddd$	$P\bar{1}$	$P2_1/n$	$C2/c$	$P\bar{1}$
radiation	Mo Kα	Mo Kα	Mo Kα	Mo Kα	Mo Kα
T (K)	173	253	233	298	233
μ (mm^{-1})	1.610	1.289	2.560	1.772	1.451
2θ range (deg)	2–60	2–60	2–55	2–53	2–45
no. of coll, indep reflects	4800	4198	5310	5341	8166
no. of obs reflects ($I > 3\sigma$)	4492	2818	3515	2870	5579
no. of variables	253	190	343	343	338
R	0.0574	0.0532	0.0538	0.0599	0.0983
R_w	0.0679	0.0533	0.0584	0.0575	0.0983

for $[(tfd)Cu(OCH_2CH_2OMe)]_n$, 584 ($n$ = 2) and 1167 (n = 4)). MS: 722 ($[M]^+/2 + Cu + (OCH_2CH_2OMe)$, $^{63}Cu/^{63}Cu/^{65}Cu$), 647 ($[M]^+/2 + Cu$), $[M]^+/2$ was not observed, 553 ($[M]^+/2 - (OMe)$, $^{63}Cu/^{65}Cu$), 509 ($[M]^+/2 - (OCH_2CH_2OMe)$), 478 ($[M]^+/2 - (OCH_2CH_2OMe) - (OMe)$), 434 ($[M]^+/2 - 2(OCH_2CH_2OMe)$), 430 ($[M]^+/2 - (tfd)$), 371 ($[M]^+/2 - 2(OCH_2CH_2OMe) - Cu$, ^{65}Cu), 355 ($[M]^+/2 - (OCH_2CH_2OMe) - (tfd)$, $^{63}Cu/^{65}Cu$). IR: 1624 (vs, $\nu_{(C=O)}$), 1522 (m), 1300 (vs), 1225 (m), 1193 (m), 1147 (s), 1140 (s), 1075 (m), 1063 (m), 1022 (w).

Tetrakis[μ_3-(2-methoxyethoxy)]tetrakis[(1,1,1,5,5,5-hexafluoro-2,4-pentanedionato)copper(II)] ($[(hfd)Cu(OCH_2CH_2OMe)]_4$ (14). **14** was prepared as described for **13**, starting from **3**: grass green solid; yield 95%; mp 187–189 °C; dec >225 °C; subl 105 °C 10^{-1} Torr. **14** is very slightly soluble in 2-methoxyethanol, moderately soluble in hexane, more soluble in ether, and very soluble in THF, $CHCl_3$, and CH_2Cl_2. Dark green single crystals suitable for X-ray diffraction could be obtained by cooling slowly a hot saturated solution of **14** in hexane to room temperature. Anal. Calcd for $C_{16}H_{16}F_{12}O_8Cu_2$: C, 27.80; H, 2.33; F, 32.98; Cu, 18.38. Found: C, 27.52; H, 2.36; F, 32.87; Cu, 17.00. Vis: THF, 700 (46); $CHCl_3$, 668 (100). M_r: found, 1342 (calcd for $[(hfd)Cu(OCH_2CH_2OMe)]_4$, 1342). MS: 829 ($[M]^+/2 + Cu + (OCH_2CH_2OMe)$, $^{63}Cu/^{63}Cu/^{65}Cu$), 754 ($[M]^+/2 + Cu$), 691 ($[M]^+/2$, $^{63}Cu/^{65}Cu$), 660 ($[M]^+/2 - (OMe)$), 616 ($[M]^+/2 - (OCH_2CH_2OMe)$), 585 ($[M]^+/2 - (OCH_2CH_2OMe) - (OMe)$), 541 ($[M]^+/2 - 2(OCH_2CH_2OMe)$), 485 ($[M]^+/2 - (hfd)$), 478 ($[M]^+ - 2(OCH_2CH_2OMe) - Cu$, ^{65}Cu), 410 ($[M]^+/2 - (OCH_2CH_2OMe) - (hfd)$, $^{63}Cu/^{65}Cu$). IR: 1649 (s, $\nu_{(C=O)}$), 1559 (m), 1531 (w), 1482 (m), 1260 (s), 1221 (m), 1196 (s), 1149 (vs), 1111 (m), 1060 (m), 1021 (w).

Bis(μ_3-(2-methoxyethoxy))bis(μ-(2-methoxyethoxy))bis((2-methoxyethoxy))tetrakis[(2,2,6,6-tetramethyl-3,5-heptanedionato)copper(II)]-barium(II) ($BaCu_4(thd)_4(OCH_2CH_2OMe)_6$) (15). Method a. To a solution of 2.5 g (2.0 mmol) of **12** in 30 mL of 2-methoxyethanol was added at 0 °C dropwise bis(2-methoxyethoxy)barium (prepared from 0.6 g (3.9 mmol) of Ba in 15 mL of 2-methoxyethanol). After 1 h the resulting solution was warmed to room temperature. A blue precipitate was noticed and dissolved by warming to 60 °C. Dark blue crystals were obtained by slowly cooling to –30 °C, collected by filtration, and dried in vacuo. The filtrate was concentrated to half its volume and slowly cooled to –30 °C. The resulting dark blue single crystals, suitable for X-ray diffraction, were collected by filtration and dried in vacuo: total yield 55%; mp 113–119 °C; dec >175 °C. Anal. Calcd for $C_{62}H_{118}O_{20}BaCu_4$: Ba, 8.72; Cu, 16.14. Found: Ba, 8.28; Cu, 17.16.

Method b. Use of 2.5 g (2.0 mmol) of **12** and 0.3 g (2.0 mmol) of Ba in the procedure described above gave the same: yield 50%; mp 113–119 °C; dec >175 °C. Anal. Calcd for $C_{62}H_{118}O_{20}BaCu_4$: C, 47.28; H, 7.55; Ba, 8.72; Cu, 16.14. Found: C, 46.63; H, 7.54; Ba, 8.18; Cu, 16.06. Vis: $CHCl_3$, 650, 533. IR: 1589 (s), 1572 (s), 1553 (m), 1534 (s), 1504 (s), 1402 (vs), 1359 (s), 1244 (m), 1226 (m), 1196 (m), 1181 (s), 1147 (m), 1124 (s), 1085 (s), 1078 (s), 1020 (m), 912 (w), 895 (m), 873 (ms), 834 (m), 791 (m), 762 (w), 743 (w).

X-ray Structure Determination

Diffraction data were collected on Nicolet R3m (**6**, **10**, **12**, **15**) and CAD-4 (**14**) four-circle diffractometers using Mo Kα radiation with a graphite monochromator. All studied compounds (with the exception of **14**) are unstable and were placed in glass capillaries for the measurement of intensities. In the case of compounds **6** and **10** mother liquor had to be placed into the capillaries, because of potential loss of solvent molecules. The lattice parameters were based on 24 centered reflections with 2θ values between 25 and 28° (**6**, **10**, **12**, **15**) and 25 with 2θ values between 16.4 and 22.8° (**14**). The $\theta/2\theta$-scan (**6**, **10**, **15**) and ω-scan techniques (**12**, **14**) were used to record the intensities of reflections. The structures were solved by automated direct (**6**, **10**, **15**) and heavy-atom methods (**12**, **14**) and refined by full-matrix least squares in anisotropic approximation for non-hydrogen atoms. In **15** only the metal and oxygen atoms were refined anisotropically. The hydrogen atoms, whose positions were reassigned geometrically at every stage of refinement, were included in the refinement of all structures (with the exception of **15**) with fixed values of isotropic thermal parameters. No absorption correction was applied. The instability of the crystals of **15** did not allow us to collect reflections after 2θ = 45° and to refine the structure anisotropically for all non-hydrogen atoms. The refinement of **10**, **14**, and **15** in the centrosymmetric space groups led to results satisfactory for the structural and chemical description of these compounds. There were no indications of the necessity of refinement in the noncentrosymmetric space groups, which (especially for **15**) would require a much larger number of collected reflections. The crystallographic data for compounds **6**, **10**, **12**, **14**, and **15** are given in Table I, and positional and thermal parameters of atoms are listed in Tables II–VI. Selected bond lengths and angles are given in Tables VII–XVI. All calculations were performed on a Micro-Vax 2000 computer using the SHELX-PLUS program package.[9]

Results and Discussion

The present work is part of systematic investigations in the field of synthesis and the study of properties of alkaline earth, copper, and yttrium mixed-metal complexes for potential use in chemical deposition of oxide materials. Out of the series of complexes **4**–**15** (Chart I), the X-ray analyses of compounds **6**, **10**, **12**, **14**, and **15** are carried out to study the ligand influence on the specific arrangement of certain complex fragments in the solid state. **6** and **10** are structurally characterized as complexes with four (**6**) and two (**10**) solvated THF molecules, which coordinate the Cu atoms.

The five structurally investigated Cu complexes **6**, **10**, **12**, **14**, and **15** belong to four different structural types: a binuclear system like **10**, the tetranuclear cubane structures like **6** and **14**,

---

(9) Sheldrick, G. M. *SHELXTL-PLUS, Crystallographic System*, Version 2; Nicolet XRD Corp.: Madison, WI, 1988.

Table II. Atomic Coordinates (×10^4) and Equivalent Isotropic Displacement Coefficients (Å^2 × 10^3) in Structure 6

	x	*y*	*z*	*U*(eq)^a
Cu	500 (1)	882 (1)	1690 (1)	28 (1)
F(1)	742 (4)	−721 (1)	1935 (3)	160 (3)
F(2)	−36 (7)	−781 (2)	1365 (2)	192 (4)
F(3)	−674 (5)	−848 (1)	1987 (3)	217 (4)
F(4)	−3021 (3)	526 (3)	1637 (3)	247 (5)
F(5)	−2747 (4)	597 (3)	2283 (2)	223 (4)
F(6)	−2631 (3)	1150 (2)	1884 (3)	192 (4)
O(1)	1875 (2)	925 (1)	1644 (1)	29 (1)
O(2)	475 (2)	177 (1)	1683 (1)	39 (1)
O(3)	−888 (2)	925 (1)	1749 (1)	41 (1)
O(4)	504 (3)	734 (1)	2552 (1)	61 (1)
C(1)	−260 (3)	−64 (1)	1756 (1)	43 (1)
C(2)	−1178 (3)	85 (2)	1828 (2)	50 (1)
C(3)	−1417 (3)	571 (2)	1814 (1)	42 (1)
C(4)	−58 (4)	−615 (2)	1756 (2)	70 (2)
C(5)	2462 (3)	718 (2)	1905 (2)	60 (2)
C(6)	2505 (3)	594 (1)	1869 (1)	41 (1)
C(7)	872 (4)	329 (2)	2793 (2)	67 (2)
C(8)	119 (6)	183 (3)	3113 (3)	107 (3)
C(9)	−460 (7)	629 (3)	3190 (3)	128 (4)
C(10)	−108 (4)	988 (2)	2849 (2)	72 (2)

^{a} Equivalent isotropic *U* defined as one-third of the trace of the orthogonalized $\mathbf{U}_{ij}$ tensor.

Table III. Atomic Coordinates (×10^4) and Equivalent Isotropic Displacement Coefficients (Å^2 × 10^3) in Structure **10**

	x	*y*	*z*	*U*(eq)^a
Cu	740 (1)	3884 (1)	4471 (1)	45 (1)
F(1)	54 (8)	−1686 (5)	2578 (9)	229 (5)
F(2)	−1772 (6)	−1168 (5)	2498 (6)	152 (3)
F(3)	−304 (9)	−742 (6)	1248 (6)	192 (4)
F(4)	2826 (4)	8611 (4)	5403 (3)	77 (2)
F(5)	5404 (5)	10608 (4)	7023 (5)	112 (2)
F(6)	6453 (4)	9984 (5)	9062 (5)	117 (2)
F(7)	4865 (5)	7304 (5)	9437 (4)	101 (2)
F(8)	2268 (4)	5293 (4)	7828 (3)	75 (2)
O(1)	1166 (4)	5880 (3)	5751 (3)	51 (1)
O(2)	2562 (4)	3832 (4)	5137 (4)	57 (2)
O(3)	−104 (4)	1797 (3)	3379 (4)	57 (2)
O(4)	1731 (5)	4645 (5)	2786 (4)	75 (2)
C(1)	544 (6)	905 (5)	3380 (6)	56 (2)
C(2)	1891 (7)	1228 (6)	4092 (6)	68 (3)
C(3)	2860 (6)	2677 (6)	4935 (6)	56 (2)
C(4)	4310 (7)	2927 (8)	5689 (7)	83 (4)
C(5)	−348 (9)	−669 (7)	2430 (9)	86 (4)
C(6)	2461 (5)	6895 (5)	6577 (5)	44 (2)
C(7)	3290 (6)	8268 (6)	6410 (5)	54 (2)
C(8)	4624 (7)	9299 (6)	7249 (7)	68 (3)
C(9)	5156 (6)	8977 (7)	8243 (6)	71 (3)
C(10)	4367 (6)	7636 (7)	8442 (6)	65 (3)
C(11)	3029 (6)	6610 (6)	7605 (5)	54 (2)
C(12)	1629 (8)	5848 (8)	2407 (7)	84 (4)
C(13)	2112 (12)	5734 (11)	1165 (9)	126 (6)
C(14)	2549 (15)	4528 (10)	790 (9)	154 (7)
C(15)	2154 (13)	3736 (9)	1754 (8)	128 (6)

^{a} Equivalent isotropic *U* defined as one-third of the trace of the orthogonalized $\mathbf{U}_{ij}$ tensor.

Table IV. Atomic Coordinates (×10^4) and Equivalent Isotropic Displacement Coefficients (Å^2 × 10^3) in Structure **12**

	x	*y*	*z*	*U*(eq)^a
Cu(1)	683 (1)	619 (1)	4435 (1)	29 (1)
Cu(2)	−290 (1)	−948 (1)	3684 (1)	33 (1)
O(1)	891 (4)	1742 (3)	4000 (3)	40 (2)
O(2)	−113 (4)	−2144 (3)	3879 (3)	43 (2)
O(3)	−973 (4)	−1142 (3)	2674 (3)	46 (2)
O(4)	1732 (4)	849 (3)	5294 (2)	34 (2)
O(5)	−296 (4)	265 (3)	3587 (3)	41 (2)
O(6)	571 (3)	−633 (3)	4627 (2)	30 (1)
O(7)	2557 (5)	−178 (4)	4044 (3)	61 (2)
O(8)	−125 (7)	1114 (5)	1670 (4)	106 (4)
C(1)	1734 (6)	2176 (5)	4116 (4)	40 (2)
C(2)	2547 (6)	1997 (5)	4687 (4)	44 (3)
C(3)	2505 (6)	1361 (4)	5239 (4)	33 (2)
C(4)	−344 (7)	−2751 (5)	3408 (4)	43 (3)
C(5)	−780 (7)	−2637 (5)	2654 (4)	53 (3)
C(6)	−1071 (6)	−1856 (5)	2331 (4)	44 (3)
C(7)	1541 (6)	−1093 (4)	4805 (4)	36 (2)
C(8)	2286 (7)	−1039 (6)	4166 (5)	51 (3)
C(9)	3062 (8)	−29 (7)	3362 (5)	71 (4)
C(10)	−606 (6)	733 (5)	2913 (3)	39 (2)
C(11)	240 (7)	663 (6)	2339 (4)	57 (3)
C(12)	638 (13)	1090 (10)	1104 (7)	146 (8)
C(13)	−118 (9)	−3646 (5)	3724 (5)	60 (3)
C(14)	−1088 (17)	−3968 (11)	4010 (14)	321 (20)
C(15)	109 (18)	−4269 (9)	3191 (8)	236 (14)
C(16)	618 (20)	−3650 (8)	4353 (12)	385 (21)
C(17)	−1602 (8)	−1808 (6)	1507 (5)	57 (3)
C(18)	−2688 (12)	−1766 (17)	1525 (7)	303 (20)
C(19)	−1272 (17)	−1038 (11)	1120 (7)	222 (13)
C(20)	−1335 (16)	−2487 (11)	1015 (7)	210 (12)
C(21)	1875 (7)	2923 (5)	3551 (5)	50 (3)
C(22)	2581 (11)	2607 (7)	2959 (6)	102 (5)
C(23)	2407 (10)	3706 (6)	3929 (6)	95 (5)
C(24)	800 (8)	3186 (6)	3200 (7)	90 (5)
C(25)	3467 (6)	1257 (5)	5838 (4)	44 (3)
C(26)	4490 (8)	1222 (9)	5434 (6)	109 (6)
C(27)	3347 (8)	464 (7)	6317 (6)	83 (4)
C(28)	3479 (9)	2047 (7)	6360 (6)	90 (5)

^{a} Equivalent isotropic *U* defined as one-third of the trace of the orthogonalized $\mathbf{U}_{ij}$ tensor.

a ladderlike tetranuclear unit of **12**, and mixed-metal complex **15**, which comprises two binuclear Cu, O moieties.

Dimer $Cu_2C_{30}H_{24}F_{16}O_8$ (10). Each Cu atom of the centrosymmetrical dimer **10** (Figure 1) has a typical square-pyramidal surrounding[6,10] with the O(4) atom of the THF molecule in the apical position. In other terms, **10** has a basal-edged pyramidal geometry and could be classified as type III according to the systematics of four- and five-coordinated dinuclear copper(II) complexes.[10] The Cu atom deviates from the plane of four basal atoms O(1), O(1a), O(2), and O(3) (maximum deviation is 0.009 Å) by 0.175 Å toward the apical O(4) atom. The basal plane O(1), O(1a) O(2), and O(3) is practically coplanar with the central four-membered ring Cu, O(1), Cu(a), O(1a) (the dihedral angle is 6.6°) and nearly coplanar with the mean plane of the six-membered chelate ring (the dihedral angle is 11.2°). The latter is slightly distorted toward a boat form; the planes O(2), Cu, O(3) and C(1), C(2), C(3) are bent to one side relative to the plane of the bottom at the dihedral angles of 4.6 and 2.9°, respectively. The basal Cu–O distances in the four-membered ring of 1.934 and 1.939 (3) Å are slightly shorter than in the six-membered chelate ring (1.954 and 1.955 (3) Å). The average basal Cu–O distance of 1.945 Å in **10** is very close to the corresponding reference value of 1.930 Å, e.g. in the structure of $Cu_2(C_{25}H_{20}O_2P)_2 \cdot (CH_3O)_2$ (**16**), in which the molecule also forms the centrosymmetrical dimer and the Cu atom adopts a comparable square-pyramidal surrounding of five oxygen atoms.[11] The apical Cu···O(THF) distance of 2.441 (3) Å in **10** is longer than the Cu···O(CH_3) distance of 2.42 (1) Å in **16**. This separation varies in dimeric complexes with pentacoordinated Cu centers in a broad range from practically an equal length in basal bonds to nearly 2.92 Å, which is the sum of radii on the Cu atom (1.40 Å) in a nonbonded state and the intermolecular contact limit of the O atom (1.52 Å)[12] (e.g. 2.897 (8) Å in $Cu_2(C_6H_{14}NO)_2(C_7H_5O_2Br_2)_2$).[13] The presence of C_6F_5 acceptor substituents at the O-atoms in the central four-membered ring does not lead to an essential increase in Cu···Cu′ separations in **10** (3.070 (2) vs 2.982 (3)–3.348 Å in other dimeric Cu complexes[5]). The Cu···Cu

---

(10) Smollander, K. *Acta Chem. Scand.* **1983**, *200A*, 1.

(11) Wrobleski, D. A.; Rauchfuss, T.; Rheingold, A. L.; Lewis, K. A. *Inorg. Chem.* **1984**, *23*, 3124.

(12) Bondi, A. J. *J. Phys. Chem.* **1964**, *68*, 441.

(13) Smollander, K. *Inorg. Chim. Acta* **1987**, *133*, 317.

Table V. Atomic Coordinates ($\times 10^4$) and Equivalent Isotropic Displacement Coefficients ($Å^2 \times 10^3$) in Structure **14**

	x	y	z	U(eq)[a]
Cu(1)	813 (1)	1324 (1)	2826 (1)	67 (1)
Cu(2)	−336 (1)	2791 (1)	3252 (1)	69 (1)
O(1)	1844 (3)	1440 (4)	2404 (3)	76 (2)
O(2)	1281 (4)	1148 (4)	3843 (3)	81 (3)
O(3)	−251 (3)	1377 (3)	3160 (3)	63 (2)
O(4)	−947 (5)	−50 (5)	2859 (4)	114 (4)
O(5)	681 (3)	2714 (3)	2819 (3)	66 (2)
O(6)	350 (5)	4092 (5)	3532 (5)	107 (4)
O(7)	−1360 (4)	3126 (4)	3560 (3)	82 (3)
O(8)	61 (4)	2629 (4)	4316 (3)	78 (2)
C(1)	2490 (5)	1380 (6)	2772 (5)	70 (3)
C(2)	2616 (5)	1219 (6)	2548 (5)	81 (4)
C(3)	1998 (6)	1130 (6)	4012 (5)	75 (4)
C(4)	3189 (6)	1484 (9)	2300 (8)	99 (5)
F(1)	3808 (5)	1105 (6)	2572 (5)	168 (5)
F(2)	3443 (6)	2196 (7)	2378 (6)	202 (6)
F(3)	3081 (4)	1342 (8)	1621 (4)	208 (7)
C(5)	2199 (8)	1016 (11)	4865 (6)	112 (6)
F(4)	2087 (7)	1628 (7)	5239 (4)	222 (7)
F(5)	1776 (5)	463 (6)	5132 (4)	161 (5)
F(6)	2924 (5)	784 (6)	5013 (4)	169 (5)
C(6)	−517 (5)	897 (6)	3755 (4)	73 (4)
C(7)	−475 (6)	58 (7)	3540 (5)	93 (5)
C(8)	−1251 (16)	−705 (13)	2755 (10)	287 (15)
C(9)	1297 (6)	3191 (6)	3166 (5)	77 (4)
C(10)	1062 (7)	4022 (7)	3179 (6)	89 (4)
C(11)	180 (8)	4807 (8)	3761 (8)	133 (7)
C(12)	−1524 (6)	3247 (6)	4236 (5)	76 (4)
C(13)	−1061 (6)	3122 (6)	4893 (5)	81 (4)
C(14)	−317 (6)	2822 (6)	4878 (4)	74 (4)
C(15)	−2337 (8)	3594 (10)	4293 (7)	110 (6)
F(7)	−2546 (5)	3678 (7)	4969 (4)	198 (5)
F(8)	−2876 (5)	3186 (7)	3945 (6)	184 (6)
F(9)	−2387 (5)	4263 (6)	3946 (5)	171 (5)
C(16)	140 (9)	2662 (12)	5614 (6)	119 (7)
F(10)	127 (10)	1950 (8)	5779 (7)	266 (9)
F(11)	816 (6)	2816 (10)	5638 (4)	251 (9)
F(12)	−146 (6)	2972 (9)	6186 (4)	240 (7)

[a] Equivalent isotropic U defined as one-third of the trace of the orthogonalized U_{ij} tensor.

distance depends on the extent of coupling of Cu atoms; see e.g. ref 14. The interaction of the C_6F_5 substituents with the Cu_2O_2 ring should be considered of mainly σ-type especially when the large dihedral angle between their planes of 67.1° is taken into account. This angle is probably governed by intramolecular noncovalent interactions of the F substituents with the Cu and O framework atoms. The distribution of intramolecular noncovalent contacts of the F atoms F(4) and F(8) (F(4)$\cdots$Cu′ = 3.462 Å, F(4)$\cdots$C(12) = 3.410 Å, F(8)$\cdots$Cu = 3.514 Å, F(8)$\cdots$O(2) = 2.928 Å) also indicates a blocking action of the C_6F_5 substituents on the potential sixth coordination site of the Cu atom and explains the observed small asymmetry of the exocyclic bond angles at the O(1) atom (CuO(1)C(6) = 129.4 (3)°, Cu′O(1)C(6) = 127.2 (3)°). The presence of the bulky C_6F_5 substituents prevents the dimers **10** from further association with formation of a tetranuclear structure. The essentially planar coordination of the bridged oxygen atoms of the Cu_2O_2 ring is remarkable (the sum of bond angles at the O(1) atom is 360.0°). The length of the exocyclic O(1)–C(6) bond of 1.351 (5) Å appears only slightly smaller than e.g. 1.370 Å in aryl alkyl ethers,[15] which confirms the absence of any essential π-interactions between the fluorinated phenyl ring and the π-electron system of the Cu_2O_2 ring of **10**. The value of 103.4 (1)° of the CuO(1)Cu′ bridge bond angle lies within the expected broad interval of 86.3 (1)–115 (1)° in binuclear Cu(II) complexes with a Cu_2O_2 core.[6]

Tetramers $Cu_4C_{40}H_{48}F_{24}O_{16}$ (6) and $Cu_4C_{32}H_{32}F_{24}O_{16}$ (14). Both the tetrameric cubane complexes **6** and **14** occupy special unit cell positions with the crystallographic 222 and 2 symmetry, respectively (Figures 2 and 3). The Cu atoms are in both cases six-coordinated and have a distorted (especially in **14**) square-pyramidal [4 + 2] environment. Both complexes possess the so-called type I Cu_4O_4 core in which the four stretched intracore Cu$\cdots$O bonds are parallel.[5,10] The different nature of the residues at the bridging O atoms in **6** and **14** leads to some structural differences. The O(4) and O(6) atoms of the 2-methoxyethoxide moieties in **14** can provide additional bonding to the sixth coordination site of the Cu atoms, which are occupied in **6** by the solvent THF. Judging from the corresponding Cu$\cdots$O distances, this secondary coordinative interaction is in **6** somewhat stronger than in **14** (in **6**, Cu$\cdots$O(4) = 2.547 (4) Å; in **14**, Cu(1)$\cdots$O(4) = 2.672 (8) Å and Cu(2)$\cdots$O(6) = 2.560 (8) Å). However, the average intracore bond contact trans to the extracore Cu$\cdots$O interactions is in **14** (2.423 Å) slightly stronger than in **6** (2.441 (3) Å). Since the natures of the basal ligand systems in **6** and **14** are chemically very similar, the average Cu–O(basal) bond lengths are practically equal (1.945 and 1.949 Å, respectively).

As denoted, the deviation Δ of the Cu atoms from the basal plane or the deformation of the axial O$\cdots$Cu$\cdots$O moiety from linearity can be used to characterize the distortion of the square-bipyramidal Cu coordination. The Δ values in **6** (0.027 Å out of the cage) and in **14** (0.013 Å toward and 0.016 Å out of the cage for Cu(1) and Cu(2), respectively) are not significant. The deviations from linearity of the axial O$\cdots$Cu$\cdots$O units are in **14** much larger (152.8 (2) and 148.8 (2)° for Cu(1) and Cu(2), respectively) than in the more symmetric complex **6** (172.3 (1)°).

The observed remarkable tetrahedral distortion of the equatorial surrounding of the Cu atoms in **6** and especially in **14** (the deviations of O atoms from the equatorial planes are 0.049, −0.043, 0.044, −0.050 Å in **6** and 0.216, −0.191, 0.196, −0.220 Å and 0.113, −0.113, 0.126, −0.126 Å for the Cu(1) and Cu(2) atoms in **14**) can be explained by rehybridization of the bridging O atoms on formation of the Cu_4 units. The absence of shortened intramolecular contacts between the "upper" and "lower" dimeric parts of **6** and **14** is remarkable. Moreover, the joining of two dimers into the tetrameric unit may be understood as a way to minimize steric hindrance: the interdimeric noncovalent distances O(2)$\cdots$C(6) = 3.117 Å and O(3)$\cdots$C(6) = 3.011 Å (average 3.064 Å) in **6** and O(1)$\cdots$(6) = 3.100 Å, O(2)$\cdots$C(6) = 3.091 Å, O(7)$\cdots$C(9) = 3.054 Å, and O(8)$\cdots$C(9) = 3.164 Å (average 3.102 Å) in **14** are somewhat larger than O(2)$\cdots$C(6) = 3.054 Å and O(3)$\cdots$C(6) = 3.026 Å (average 3.040 Å) in **10** due to the mentioned tetrahedral distortion of the basal Cu coordination planes and rehybridization of the bridging oxygen atoms.

During this rehybridization the ideally planar coordination of the bridging O(1) in **10** changes to a pyramidal coordination in **6** (the deviation of the O(1) atom from the plane Cu, Cu′, C(6) toward the Cu atom participating the coordination Cu$\cdots$O(1) bond is 2.13 Å) and to an almost pyramidal geometry in **14** (the displacements of the O(3) and O(5) atoms toward Cu atoms are 0.452 and 0.470 Å, respectively). While **6** and **10** show smaller distortions from planarity of the "dimeric" Cu_2O_2 rings, we find a pronounced nonplanarity in **14** (the deviations of atoms from the mean planes Cu(1), O(3), Cu(1′), O(3′) and Cu(2), O(5), Cu(2′), O(5′) are −0.045, 0.045, −0.045, 0.045 Å and 0.066, −0.066, 0.066, −0.066 Å) accompanied by a larger pyramidalization at the Cu centers.

Tetramer $Cu_4C_{56}H_{104}O_{16}$ (12). The Cu, O framework of the centrosymmetrical complex **12** (Figure 4) represents an example of a less common double-chain ladderlike tetranuclear Cu complex.[3,10,16,17] Moreover, **12** represents the first example of

---

(14) Karlin, K. D.; Farooq, A.; Hayes, J. C.; Cohen, B. I.; Rowe, T. M.; Sinn, E.; Zubieta, J. *Inorg. Chem.* **1987**, *26*, 1271.

(15) Allen, F. H.; Kennard, O.; Watson, D. G.; Brammer, L.; Orpen, A. G. *J. Chem. Soc., Perkin Trans. 2* **1987**, S1.

(16) Andrew, J. E.; Blake, A. B. *J. Chem. Soc., Dalton Trans.* **1973**, 1102.

(17) Barraclough, C. G.; Brookes, R. W.; Martin, R. L. *Aust. J. Chem.* **1974**, *27*, 1843.

Table VI. Atomic Coordinates (×10⁴) and Equivalent Isotropic Displacement Coefficients (Å² × 10³) in Structure **15**

	x	*y*	*z*	*U*(eq)[a]		*x*	*y*	*z*	*U*(eq)[a]
Ba(1)	1076 (1)	4971 (1)	2560 (1)	48 (1)	C(19)	4822 (21)	3529 (17)	1450 (15)	71 (8)
Cu(1)	2960 (2)	3460 (2)	2029 (2)	52 (1)	C(20)	4580 (22)	3176 (18)	889 (16)	84 (9)
Cu(2)	1777 (2)	2791 (2)	3240 (2)	60 (1)	C(21)	3706 (20)	2885 (15)	798 (13)	56 (7)
Cu(3)	962 (2)	7156 (2)	1860 (2)	54 (1)	C(22)	3599 (20)	2457 (17)	224 (14)	67 (8)
Cu(4)	2508 (2)	6493 (2)	2969 (2)	53 (1)	C(23)	3728 (26)	3047 (22)	−482 (18)	131 (14)
O(1)	2736 (10)	3907 (9)	2853 (8)	52 (7)	C(24)	2707 (24)	2186 (22)	235 (19)	128 (13)
O(2)	2319 (13)	4920 (11)	3824 (8)	70 (8)	C(25)	4235 (24)	1649 (21)	338 (18)	121 (13)
O(3)	2329 (10)	6030 (9)	2173 (8)	49 (7)	C(26)	5775 (23)	3806 (20)	1499 (17)	86 (9)
O(4)	2119 (12)	5029 (11)	1200 (8)	64 (8)	C(27)	5752 (29)	4708 (24)	1203 (22)	157 (17)
O(5)	586 (12)	3503 (10)	3324 (9)	67 (8)	C(28)	6501 (30)	3316 (27)	1127 (23)	179 (19)
O(6)	−406 (14)	5004 (12)	3548 (11)	90 (9)	C(29)	6076 (25)	3614 (23)	2202 (18)	129 (14)
O(7)	14 (12)	6467 (10)	1849 (9)	66 (7)	C(30)	3492 (21)	1586 (17)	3558 (15)	67 (8)
O(8)	−529 (13)	4933 (11)	1681 (12)	95 (10)	C(31)	3312 (23)	1399 (19)	4293 (16)	90 (10)
O(9)	1715 (11)	3245 (10)	2178 (9)	64 (7)	C(32)	2508 (25)	1799 (21)	4585 (18)	91 (10)
O(10)	1182 (14)	1624 (12)	2764 (11)	91 (10)	C(33)	2371 (33)	1515 (27)	5414 (23)	133 (14)
O(11)	1151 (11)	6678 (10)	2867 (8)	58 (7)	C(34)	1946 (28)	2346 (24)	5636 (21)	151 (16)
O(12)	14 (14)	8281 (11)	2403 (12)	92 (10)	C(35)	3217 (36)	1233 (35)	5771 (29)	262 (31)
O(13)	4208 (13)	3690 (12)	1948 (10)	78 (9)	C(36)	1704 (37)	973 (35)	5502 (30)	88 (9)
O(14)	3015 (12)	2964 (11)	1214 (9)	66 (8)	C(38)	4472 (25)	1306 (22)	2533 (17)	122 (13)
O(15)	3010 (11)	2091 (10)	3095 (9)	61 (7)	C(39)	5184 (30)	1394 (28)	3542 (23)	180 (20)
O(16)	1861 (13)	2319 (12)	4228 (9)	79 (8)	C(40)	4496 (29)	235 (24)	3608 (22)	161 (17)
O(17)	3868 (11)	6247 (11)	3010 (9)	69 (8)	C(41)	4407 (21)	6421 (17)	3462 (15)	69 (8)
O(18)	2503 (12)	7021 (12)	3764 (9)	73 (8)	C(42)	4116 (22)	6772 (17)	3982 (15)	78 (9)
O(19)	1963 (12)	7854 (10)	1889 (8)	67 (8)	C(43)	3201 (22)	7055 (17)	4106 (15)	70 (8)
O(20)	807 (12)	7644 (11)	848 (9)	70 (8)	C(44)	3011 (28)	7578 (25)	4692 (20)	112 (12)
C(1)	3441 (17)	4060 (15)	3275 (12)	58 (7)	C(45)	2355 (44)	7220 (39)	5128 (32)	332 (42)
C(2)	3066 (19)	4244 (16)	3953 (13)	64 (7)	C(46)	2740 (39)	8398 (33)	4453 (29)	270 (33)
C(3)	1945 (20)	5101 (17)	4472 (14)	80 (9)	C(47)	3685 (44)	7394 (39)	5293 (32)	333 (42)
C(4)	3071 (19)	5859 (16)	1691 (13)	66 (7)	C(48)	5484 (24)	6131 (20)	3314 (17)	90 (10)
C(5)	2632 (20)	5713 (17)	1027 (14)	72 (8)	C(49)	5683 (28)	6205 (24)	2572 (19)	144 (15)
C(6)	1732 (24)	4836 (24)	591 (19)	78 (10)	C(50)	6078 (33)	6548 (30)	3654 (25)	212 (24)
C(7)	250 (25)	3600 (22)	3983 (18)	111 (12)	C(51)	5679 (32)	5249 (26)	3583 (24)	187 (20)
C(8)	−547 (26)	4242 (23)	3959 (20)	121 (13)	C(52)	2274 (18)	8372 (15)	1376 (13)	56 (7)
C(9)	−1214 (25)	5589 (23)	3406 (20)	129 (14)	C(53)	1919 (18)	8504 (15)	706 (13)	61 (7)
C(10)	−357 (24)	6324 (21)	1203 (17)	106 (11)	C(54)	1227 (19)	8192 (16)	468 (14)	60 (7)
C(11)	−980 (25)	5683 (22)	1310 (19)	110 (12)	C(55)	886 (21)	8382 (17)	−298 (14)	73 (8)
C(12)	−1149 (25)	4360 (22)	1826 (19)	124 (13)	C(56)	899 (22)	7582 (19)	−545 (16)	99 (11)
C(13)	1161 (19)	2832 (15)	1811 (14)	65 (7)	C(57)	1434 (25)	8916 (22)	−781 (18)	125 (13)
C(14)	1438 (22)	1909 (18)	2033 (16)	87 (9)	C(58)	−119 (22)	8838 (20)	−322 (17)	106 (11)
C(15)	1449 (25)	753 (21)	3092 (18)	117 (12)	C(59)	3052 (21)	8793 (18)	1576 (15)	75 (8)
C(16)	552 (22)	7118 (18)	3298 (16)	87 (9)	C(60)	3248 (26)	8686 (23)	2305 (18)	132 (14)
C(17)	478 (21)	8084 (17)	3070 (15)	80 (9)	C(61)	3877 (32)	8433 (30)	1361 (25)	206 (23)
C(18)	−17 (24)	9112 (21)	2095 (18)	114 (12)	C(62)	2923 (28)	9676 (24)	1328 (21)	155 (16)

[a] Equivalent isotropic *U* defined as one-third of the trace of the orthogonalized $\mathbf{U}_{ij}$ tensor.

Table VII. Relevant Interatomic Distances (Å) in Structure **6**

Cu–O(1)	1.934 (3)	Cu–O(2)	1.955 (3)
Cu–O(3)	1.954 (3)	Cu–O(1a)	1.939 (3)
Cu···O(1b)	2.441 (3)	Cu···O(4)	2.547 (4)
O(2)–C(1)	1.246 (5)	O(3)–C(3)	1.245 (5)
O(1)–C(6)	1.431 (5)	O(1)–C(6)	1.431 (5)
C(1)–C(2)	1.367 (7)	C(2)–C(3)	1.391 (6)
C(1)–C(4)	1.555 (6)	C(3)–C(5)	1.542 (6)
Cu···Cua	3.282 (3)	Cu···Cub	3.318 (3)
Cu···Cuc	2.932 (3)		

Table VIII. Relevant Bond Angles (deg) in Structure **6**

O(1)–Cu–O(2)	94.6 (1)	O(1)–Cu–O(3)	172.8 (1)
O(2)–Cu–O(3)	92.5 (1)	C(3)–Cu–C(6)	142.2 (1)
O(1)–Cu–O(4)	94.5 (1)	O(2)–Cu–O(4)	81.4 (1)
O(3)–Cu–O(4)	85.7 (1)	O(1)–Cu–O(1a)	81.7 (1)
O(2)–Cu–O(1a)	92.2 (1)	O(3)–Cu–O(1a)	99.0 (1)
O(4)–Cu–O(1a)	172.3 (1)	O(1)–Cu–O(1b)	81.0 (1)
O(2)–Cu–O(1b)	173.8 (1)	O(3)–Cu–O(1b)	92.0 (1)
O(4)–Cu–O(1b)	103.2 (1)	O(1a)–Cu–O(1b)	82.8 (1)
Cu–O(1)–C(6)	122.7 (2)	Cu–O(1)–Cub	98.0 (1)
C(6)–O(1)–Cub	112.4 (2)	Cu–O(1)–Cuc	98.4 (1)
C(6)–O(1)–Cuc	123.3 (2)	Cub–O(1)–Cuc	96.4 (1)
Cu–O(2)–C(1)	123.4 (3)	Cu–O(3)–C(3)	123.8 (3)
O(2)–C(1)–C(2)	129.8 (4)	O(3)–C(3)–C(2)	128.8 (4)
C(1)–C(2)–C(3)	121.0 (4)		

Table IX. Relevant Interatomic Distances (Å) in Structure **10**

Cu–O(1)	1.952 (3)	Cu–O(2)	1.902 (4)
Cu–O(3)	1.908 (3)	Cu–O(1a)	1.960 (4)
Cu–O(4)	2.279 (5)	O(1)–C(6)	1.351 (5)
O(2)–C(3)	1.259 (8)	O(3)–C(1)	1.272 (8)
C(1)–C(2)	1.361 (9)	C(1)–C(5)	1.501 (7)
C(2)–C(3)	1.399 (9)	Cu···Cua	3.070 (2)

Table X. Relevant Bond Angles (deg) in Structure **10**

O(1)–Cu–O(2)	93.3 (1)	O(1)–Cu–O(3)	166.7 (2)
O(2)–Cu–O(3)	94.4 (2)	O(1)–Cu–O(4)	98.7 (2)
O(2)–Cu–O(4)	93.1 (2)	O(3)–Cu–O(4)	91.7 (2)
O(1)–Cu–O(1a)	76.6 (1)	O(2)–Cu–O(1a)	165.8 (2)
O(3)–Cu–O(1a)	93.8 (1)	O(4)–Cu–O(1a)	98.3 (2)
Cu–O(1)–C(6)	129.4 (3)	Cu–O(1)–Cua	103.4 (1)
Cua–O(1)–C(6)	127.2 (3)	Cu–O(2)–C(3)	126.8 (3)
Cu–O(3)–C(1)	122.5 (3)	O(3)–C(1)–C(2)	128.3 (4)
C(1)–C(2)–C(3)	124.4 (6)	O(2)–C(3)–C(2)	123.3 (6)

this type of compound with a complete 6-fold coordination of the inner Cu(1) and Cu(1a) atoms which has been studied by X-ray diffractometry. The atoms Cu(2) and Cu(2a) of **12** clearly adopt pentacoordination: the observed Cu(2)···O(8) distance of 4.753 (3) Å is too large to be of bonding significance.

Comparing **12** and **14**, one finds that they differ only in the arrangement of comparable Cu, O moieties, which are either ladder- (**12**) or columnlike (**14**).

Like in the structures of **6** and **14**, **12** shows four additional Cu···O bonds which can be described as two strongly interacting planar dimers as in **10** (e.g. "upper" and "lower" parts on Figure 4). But in contrast to the tetramers **6** and **14** the long axes of the approaching dimers are oriented parallel in **12** (Figure 5) and

Table XI. Relevant Interatomic Distances (Å) in Structure **12**

Cu(1)–O(1)	1.928 (5)	Cu(2)–O(2)	1.902 (5)
Cu(1)–O(4)	1.949 (4)	Cu(2)–O(3)	1.918 (5)
Cu(1)–O(5)	1.928 (5)	Cu(2)–O(5)	1.896 (5)
Cu(1)–O(6)	1.985 (5)	Cu(2)–O(6)	1.959 (4)
Cu(1)–O(6a)	2.326 (4)	Cu(2)–O(4a)	2.605 (5)
Cu(1)···O(7)	2.766 (6)		
O(1)–C(1)	1.254 (9)	O(2)–C(4)	1.270 (9)
O(4)–C(3)	1.257 (8)	O(3)–C(6)	1.263 (9)
C(1)–C(2)	1.40 (1)	C(4)–C(5)	1.39 (1)
C(2)–C(3)	1.38 (1)	C(5)–C(6)	1.38 (1)
Cu(1)···Cu(2)	2.986 (2)	Cu(1)···Cu(1a)	3.297 (2)
Cu(1)···Cu(2a)	3.367 (2)		

Table XII. Relevant Bond Angles (deg) in Structure **12**

O(1)–Cu(1)–O(4)	91.8 (2)	O(2)–Cu(2)–O(3)	92.7 (2)
O(1)–Cu(1)–O(5)	93.2 (2)	O(2)–Cu(2)–O(5)	172.0 (2)
O(1)–Cu(1)–O(6)	165.8 (2)	O(2)–Cu(2)–O(6)	92.6 (2)
O(1)–Cu(1)–O(6a)	112.1 (2)	O(2)–Cu(2)–O(4a)	90.8 (2)
O(1)–Cu(1)–O(7)	100.1 (2)	O(3)–Cu(2)–O(5)	94.5 (2)
O(4)–Cu(1)–O(5)	173.8 (2)	O(3)–Cu(2)–O(6)	170.6 (2)
O(4)–Cu(1)–O(6)	96.0 (2)	O(3)–Cu(2)–O(4a)	110.2 (2)
O(4)–Cu(1)–O(6a)	84.9 (2)	O(5)–Cu(2)–O(6)	79.8 (2)
O(4)–Cu(1)–O(7)	74.7 (2)	O(5)–Cu(2)–O(4a)	90.1 (2)
O(5)–Cu(1)–O(6)	78.4 (2)	O(6)–Cu(2)–O(4a)	112.0 (2)
O(5)–Cu(1)–O(6a)	96.6 (2)	Cu(1)–O(6)–Cu(1a)	99.5 (2)
O(5)–Cu(1)–O(7)	100.8 (2)	Cu(1)–O(6)–C(7)	117.6 (4)
O(6)–Cu(1)–O(6a)	80.5 (2)	Cu(2)–O(6)–Cu(1a)	103.3 (2)
O(6a)–Cu(1)–O(7)	142.2 (2)	Cu(2)–O(6)–C(7)	117.8 (4)
Cu(1)–O(1)–C(1)	123.9 (5)	Cu(1a)–O(6)–C(7)	117.0 (4)
Cu(1)–O(4)–C(3)	122.5 (4)	Cu(2)–O(2)–C(4)	126.5 (4)
O(1)–C(1)–C(2)	124.5 (7)	Cu(2)–O(3)–C(6)	126.3 (5)
O(4)–C(3)–C(2)	124.7 (6)	O(2)–C(4)–C(5)	124.5 (7)
C(1)–C(2)–C(3)	125.2 (7)	O(3)–C(6)–C(5)	124.8 (7)
Cu(1)–O(5)–Cu(2)	102.7 (2)	C(4)–C(5)–C(6)	124.8 (7)
Cu(1)–O(6)–Cu(2)	98.4 (2)	Cu(1)–O(4)–Cu(2a)	94.2 (2)
Cu(1)–O(5)–C(10)	127.5 (4)	Cu(2a)–O(4)–C(3)	125.3 (4)
Cu(2)–O(5)–C(10)	126.0 (4)		

Table XIII. Relevant Interatomic Distances (Å) in Structure **14**

Cu(1)–O(1)	1.961 (6)	Cu(2)–O(5)	1.942 (6)
Cu(1)–O(2)	1.942 (5)	Cu(2)–O(7)	1.946 (6)
Cu(1)–O(3)	1.943 (5)	Cu(2)–O(8)	1.976 (5)
Cu(1)–O(3a)	1.935 (5)	Cu(2)–O(5a)	1.948 (5)
Cu(1)···O(4)	2.672 (8)	Cu(2)···O(3)	2.445 (6)
Cu(1)···O(5)	2.402 (6)	Cu(2)···O(6)	2.560 (8)
Cu(1)···Cu(1a)	2.936 (2)	Cu(2)···Cu(2a)	2.952 (2)
Cu(1)···Cu(2)	3.309 (2)	Cu(1)···Cu(2a)	3.234 (2)

Table XIV. Relevant Bond Angles (deg) in Structure **14**

O(1)–Cu(1)–O(2)	92.2 (2)	O(7)–Cu(2)–O(8)	92.2 (2)
O(1)–Cu(1)–O(3)	170.3 (3)	O(5)–Cu(2)–O(7)	165.4 (3)
O(1)–Cu(1)–O(3a)	93.5 (2)	O(7)–Cu(2)–O(5a)	93.9 (2)
O(1)–Cu(1)–O(4)	79.3 (3)	O(7)–Cu(2)–O(6)	95.4 (3)
O(1)–Cu(1)–O(5)	89.0 (2)	O(7)–Cu(2)–O(3)	111.8 (2)
O(2)–Cu(1)–O(3)	93.8 (2)	O(5)–Cu(2)–O(8)	95.8 (2)
O(2)–Cu(1)–O(3a)	171.9 (3)	O(8)–Cu(2)–O(5a)	167.7 (3)
O(2)–Cu(1)–O(4)	103.7 (3)	O(8)–Cu(2)–O(6)	79.3 (3)
O(2)–Cu(1)–O(5)	101.1 (2)	O(3)–Cu(2)–O(8)	84.5 (2)
O(3)–Cu(1)–O(3a)	81.4 (2)	O(5)–Cu(2)–O(5a)	80.7 (2)
O(3)–Cu(1)–O(4)	106.6 (3)	O(5)–Cu(2)–O(6)	74.2 (3)
O(3)–Cu(1)–O(5)	82.3 (2)	O(3)–Cu(2)–O(5)	81.2 (2)
O(3a)–Cu(1)–O(4)	93.5 (2)	O(5a)–Cu(2)–O(6)	110.7 (3)
O(3a)–Cu(1)–O(5)	84.7 (2)	O(5a)–Cu(2)–O(3)	83.3 (2)
O(4)–Cu(1)–O(5)	152.8 (2)	O(6)–Cu(2)–O(3)	148.8 (2)

Table XV. Relevant Interatomic Distances (Å) in Structure **15**

Ba(1)–O(1)	2.71 (2)	Ba(1)–O(2)	3.02 (2)
Ba(1)–O(3)	2.68 (2)	Ba(1)–O(4)	3.01 (2)
Ba(1)–O(5)	2.73 (2)	Ba(1)–O(6)	2.85 (2)
Ba(1)–O(7)	2.77 (2)	Ba(1)–O(8)	2.89 (2)
Ba(1)–O(9)	3.08 (2)	Ba(1)–O(11)	3.01 (2)
Cu(1)–O(1)	1.90 (2)	Cu(1)–O(9)	1.88 (2)
Cu(1)–O(13)	1.88 (2)	Cu(1)–O(14)	1.93 (2)
Cu(1)···O(4)	2.81 (4)	Cu(1)···O(15)	2.70 (2)
Cu(2)–O(5)	1.94 (2)	Cu(2)–O(9)	2.03 (2)
Cu(2)–O(15)	2.00 (2)	Cu(2)–O(16)	1.91 (2)
Cu(2)···O(1)	2.45 (2)	Cu(2)···O(10)	2.55 (2)
Cu(3)–O(7)	1.90 (2)	Cu(3)–O(11)	1.95 (2)
Cu(3)–O(19)	1.98 (2)	Cu(3)–O(20)	1.96 (2)
Cu(3)···O(3)	2.45 (2)	Cu(3)···O(12)	2.53 (2)
Cu(4)–O(3)	1.89 (2)	Cu(4)–O(11)	1.92 (2)
Cu(4)–O(17)	1.92 (4)	Cu(4)–O(18)	1.93 (2)
Cu(4)···O(2)	2.81 (2)	Cu(4)···O(19)	2.73 (2)
Ba(1)···Cu(1)	3.664 (4)	Ba(1)···Cu(2)	3.525 (4)
Ba(1)···Cu(3)	3.529 (4)	Ba(1)···Cu(4)	3.676 (4)
Cu(1)···Cu(2)	3.000 (4)	Cu(3)···Cu(4)	3.002 (4)
C(13)–C(14)	1.48 (5)	C(16)–C(17)	1.55 (4)
C(19)–C(20)	1.40 (5)	C(19)–C(26)	1.51 (5)
C(20)–C(21)	1.44 (5)	C(21)–C(22)	1.47 (5)
C(22)–C(23)	1.53 (5)	C(22)–C(24)	1.42 (5)
C(22)–C(25)	1.47 (5)	C(26)–C(27)	1.47 (5)
C(26)–C(28)	1.51 (5)	C(26)–C(29)	1.39 (5)
C(30)–C(31)	1.43 (5)	C(30)–C(37)	1.56 (5)
C(31)–C(32)	1.41 (5)	C(32)–C(33)	1.60 (5)
C(33)–C(34)	1.56 (5)	C(33)–C(35)	1.37 (5)
C(33)–C(36)	1.39 (5)	C(37)–C(38)	1.46 (5)
C(37)–C(39)	1.35 (5)	C(37)–C(40)	1.48 (5)
C(41)–C(42)	1.31 (5)	C(41)–C(48)	1.59 (5)
C(42)–C(43)	1.36 (5)	C(43)–C(44)	1.56 (5)
C(44)–C(45)	1.38 (5)	C(44)–C(46)	1.32 (5)
C(44)–C(47)	1.50 (5)	C(45)–C(47)	2.02 (5)
C(48)–C(49)	1.45 (5)	C(48)–C(50)	1.43 (5)
C(48)–C(51)	1.43 (5)	C(52)–C(53)	1.36 (5)
C(52)–C(59)	1.49 (5)	C(53)–C(54)	1.31 (5)
C(54)–C(55)	1.52 (5)	C(55)–C(56)	1.49 (5)
C(55)–C(57)	1.47 (5)	C(55)–C(58)	1.51 (5)
C(59)–C(60)	1.42 (5)	C(59)–C(61)	1.36 (5)
C(59)–C(62)	1.42 (5)		

the "dimerization" proceeds via two μ_2- and μ_3-oxygen atoms, while in the cubes of **6** and **14** we find a cluster core composed of four μ_3-oxygen bridges. The interdimer separations of **12** (Cu(1)–O(6a) = 2.326 (4) Å; Cu(2)···O(4a) = 2.605 (5) Å) are significantly different from the columnlike tetramers **14**, in which the interdimer separations are practically equal (2.402 and 2.445 (6) Å).

In spite of the O(6) involvement in the inter-ring interaction, the deviation of the Cu_2O_2 ring in **12** from planarity (the individual values are 0.053, –0.055, 0.054, –0.051 Å) is nearly the same as in the two symmetrically independent Cu_2O_2 rings in **14**. The bridging O atoms of the Cu_2O_2 units in **12** have somewhat different geometries; the endocyclic bond lengths at the O(6) atom are longer (1.959 and 1.985 (5) Å) and the endocyclic bond angle is smaller (98.4 (2)°) than those parameters at the O(5) atom (1.896 and 1.928 (5) Å; 102.7 (2)°).

The distortions of the cyclic moieties of the tetramer **12** resemble those in the ladderlike analogue $Cu_4(OCH_3)_4(DPM)_4$ (**17**)[3] (DPM = dipivaloylmethane), differing only in the type of bridging substituents. The dihedral angles formed by the coordination planes O_2CuO_2 within one dimeric unit in **12** and **17** are close (16.3 and 15.6°); the bend in the inner six-membered chelate rings along the O···O line (e.g. the bend in the ring Cu(1)O(1)C(1)C(2)C(3)O(4) along the O(1)···O(4) line in **12**) is, however, essentially larger than that of the outer ones (22.6° vs 5.1° in **12**, 15.6° vs 4.8° in **17**). The main reason for the larger deformation of the inner chelate rings in **12** (and **17**) is obviously due to the partial rehybridization of the O(4) atom caused by its participation in the Cu(2a)···O(4) interaction. The basal Cu(1)–O(4) bond length of 1.949 (4) Å in **12** is found to be only slightly longer than Cu(1)–O(1) of 1.928 (4) Å, but both exceed significantly the Cu(2)–O(2) and Cu(2)–O(3) distances of 1.902 and 1.918 (5) Å in the more planar outer chelate ring. Correspondingly, the Cu(1)O(4)C(3) bond angle is slightly less than the Cu(1)O(1)C(1) ones (122.5 and 123.9 (5)°) and both are essentially less than the angles Cu(2)O(2)C(4) and Cu(2)O(3)C(6) (126.5 and 125.3 (5)°). The contribution of the noncovalent intramolecular steric interactions in the deformation of the inner chelate ring of **12** is probably less, because the deformation of the opposite outer rings is practically the same as in the tetramer **14** with a perpendicular orientation of the dimer moieties.

Table XVI. Relevant Bond Angles (deg) in Structure **15**

O(1)–Ba(1)–O(2)	57.7 (5)	O(1)–Ba(1)–O(3)	78.5 (5)
O(2)–Ba(1)–O(3)	71.3 (5)	O(1)–Ba(1)–O(4)	72.2 (5)
O(3)–Ba(1)–O(4)	58.7 (5)	O(1)–Ba(1)–O(5)	75.5 (5)
O(2)–Ba(1)–O(5)	85.3 (5)	O(3)–Ba(1)–O(5)	151.7 (5)
O(4)–Ba(1)–O(5)	121.7 (5)	O(1)–Ba(1)–O(6)	122.4 (5)
O(2)–Ba(1)–O(6)	83.3 (5)	O(3)–Ba(1)–O(6)	130.3 (5)
O(4)–Ba(1)–O(6)	162.2 (5)	O(5)–Ba(1)–O(6)	59.3 (5)
O(1)–Ba(1)–O(7)	151.4 (5)	O(2)–Ba(1)–O(7)	121.2 (5)
O(3)–Ba(1)–O(7)	74.9 (5)	O(4)–Ba(1)–O(7)	85.0 (5)
O(5)–Ba(1)–O(7)	132.5 (5)	O(6)–Ba(1)–O(7)	83.6 (5)
O(1)–Ba(1)–O(8)	139.4 (5)	O(2)–Ba(1)–O(8)	162.4 (5)
O(3)–Ba(1)–O(8)	123.0 (5)	O(4)–Ba(1)–O(8)	83.1 (5)
O(5)–Ba(1)–O(8)	83.3 (5)	O(6)–Ba(1)–O(8)	79.3 (5)
O(7)–Ba(1)–O(8)	59.9 (5)	O(1)–Ba(1)–O(9)	50.3 (5)
O(2)–Ba(1)–O(9)	103.8 (5)	O(3)–Ba(1)–O(9)	112.2 (1)
O(4)–Ba(1)–O(9)	64.7 (5)	O(5)–Ba(1)–O(9)	57.3 (5)
O(6)–Ba(1)–O(9)	115.1 (5)	O(7)–Ba(1)–O(9)	133.5 (5)
O(8)–Ba(1)–O(9)	81.1 (5)	O(1)–Ba(1)–O(11)	113.0 (5)
O(2)–Ba(1)–O(11)	66.3 (5)	O(3)–Ba(1)–O(11)	49.8 (5)
O(4)–Ba(1)–O(11)	103.3 (5)	O(5)–Ba(1)–O(11)	81.1 (5)
O(6)–Ba(1)–O(11)	81.1 (5)	O(7)–Ba(1)–O(11)	55.0 (5)
O(8)–Ba(1)–O(11)	113.4 (5)	O(9)–Ba(1)–O(11)	160.8 (5)
O(1)–Cu(1)–O(13)	93.6 (5)	O(9)–Cu(1)–O(13)	175.6 (5)
O(1)–Cu(1)–O(14)	172.2 (5)	O(9)–Cu(1)–O(14)	90.2 (5)
O(13)–Cu(1)–O(14)	94.1 (5)	O(1)–Cu(1)–O(4)	89.4 (5)
O(4)–Cu(1)–O(9)	85.4 (5)	O(4)–Cu(1)–O(13)	95.6 (5)
O(4)–Cu(1)–O(14)	90.5 (5)	O(4)–Cu(1)–O(15)	154.0 (5)
O(5)–Cu(2)–O(9)	89.8 (5)	O(5)–Cu(2)–O(15)	176.7 (5)
O(9)–Cu(2)–O(15)	86.9 (5)	O(5)–Cu(2)–O(16)	92.1 (5)
O(9)–Cu(2)–O(16)	177.7 (5)	O(15)–Cu(2)–O(16)	91.2 (5)
O(1)–Cu(2)–O(5)	98.2 (5)	O(5)–Cu(2)–O(9)	89.8 (5)
O(5)–Cu(2)–O(10)	100.2 (5)	O(5)–Cu(2)–O(15)	176.7 (5)
O(5)–Cu(2)–O(16)	92.1 (5)	O(1)–Cu(2)–O(10)	99.5 (5)
O(5)–Cu(2)–O(10)	138.6 (5)	O(9)–Cu(2)–O(10)	76.7 (5)
O(10)–Cu(2)–O(15)	79.5 (5)	O(10)–Cu(2)–O(16)	101.7 (5)

Chart I

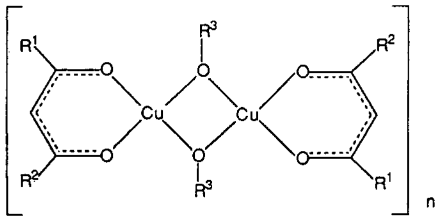

n = 1 or 2

R^1	R^2	R^3			
Bu^t	Bu^t	Me (**4**)	Pr^i (**7**)	Ph_f (**9**)	$(CH_2)_2OMe$ (**12**)
CF_3	Me	Me (**5**)	Pr^i (**8**)	Ph_f (**10**)	$(CH_2)_2OMe$ (**13**)
CF_3	CF_3	Me (**6**)	-	Ph_f (**11**)	$(CH_2)_2OMe$ (**14**)

Ph_f =

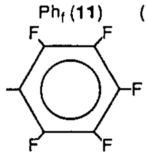

The four-membered Cu_2O_2 rings forming the Cu, O framework of the complex **12** are nearly perpendicular to each other. The corresponding symmetrically independent dihedral angles are 78.5° for Cu(1)O(5)Cu(2)O(6)/Cu(1)O(6)Cu(1a)O(6a), 96.3° for Cu(1)O(5)Cu(2)O(6)/Cu(2)O(6)Cu(2a)O(6a), and 98.7° for Cu(1)O(6)Cu(1a)O(6a)/Cu(1)O(6a)Cu(2a)O(4). The hexacoordination of the inner Cu(1) and Cu(1a) atoms of the framework of **12** is probably supporting the observed regular structure. The Cu(1) and Cu(2) atoms are practically lying in the corresponding equatorial planes; the Δ values of deviation are 0.013 and 0.089 Å, while, in the structure **17**, in which all the Cu atoms possess pentacoordination, the Δ values are essentially larger (0.05 and 0.16 Å). Despite different values for the interdimer Cu···O separations within the ladderlike Cu, O framework of **12** which nearly correspond to interbond angles at the Cu atoms (≈90°), the ladderlike Cu_2O_2 junction in **12** can be taken as an elementary unit for the construction of an infinite Cu, O double-chain structure (Figure 6). The above mentioned decrease of bond angles around the μ_3-bridged O atoms is another geometrical prerequisite for the stability of the hypothetical structure shown in Figure 6. The identity period *d* along the double chain of this polymer structure can be calculated in first approximation as the separation *d*(Cu(1)···Cu(2a)), which amounts to 3.37 Å. The determination of subcell parameters[18] of the proposed polymer structure is difficult, because of the necessity to totally reconstruct the organic environment of the Cu, O framework during the transition from **12** to the polymeric situation in Figure 6 (e.g. the exchange of bulky substituents in the chelate rings). Of course, the proposed polymer structure is

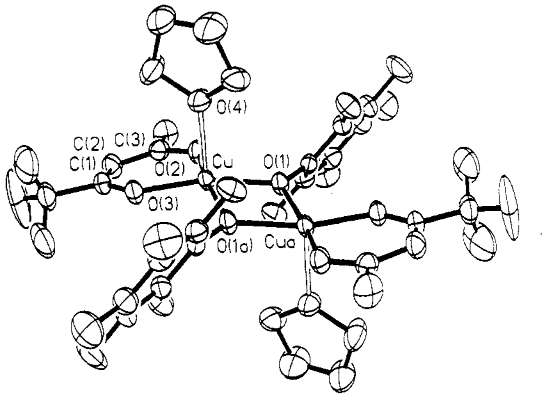

Figure 1. Structure of centrosymmetrical complex **10**. The additional Cu···O(THF) interactions are shown by open lines. The thermal ellipsoids are drawn at 50% probability.

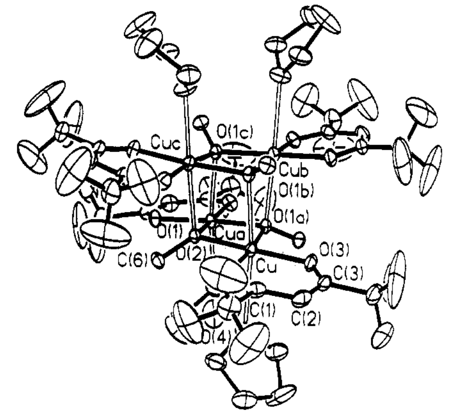

Figure 2. Structure of complex **6** (crystallographic D_2 symmetry). The additional Cu···O interactions are shown by open lines. The thermal ellipsoids are drawn at 30% probability.

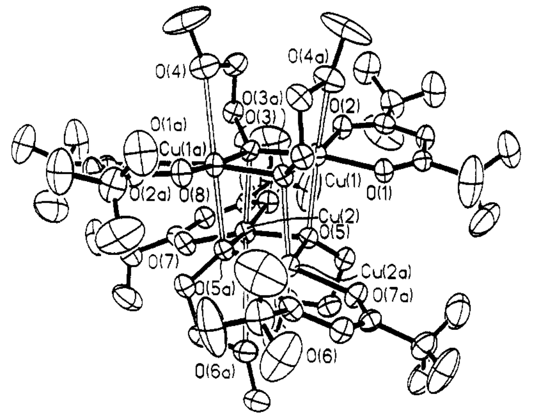

Figure 3. Structure of complex **14** (crystallographic C_2 symmetry). The additional Cu···O interactions are shown by open lines. The thermal ellipsoids are drawn at 30% probability.

---

[18] Ovchinnikov, Yu. E.; Shklover, V. E.; Struchkov, Yu. T.; Astapova, T. V.; Zhdanov, A. A. *Makromol. Chem.* **1988**, *189*, 1927.

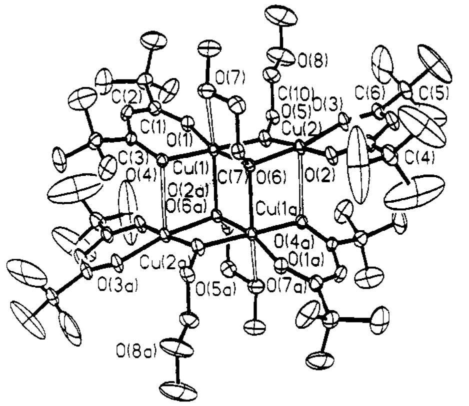

Figure 4. Structure of centrosymmetrical complex **12**. The additional Cu···O interactions are shown by open lines. The thermal ellipsoids are drawn at 30% probability.

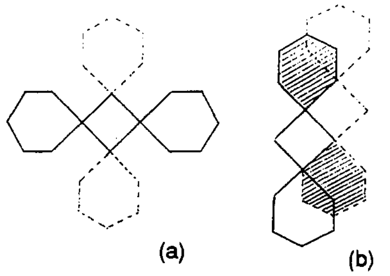

Figure 5. Two types of formation of Cu, O tetranuclear complexes from square-planar dimers: (a) The long axes of dimers are perpendicular (complexes **6** and **14**); (b) the long axes of dimers are parallel (complex **12**). The more strongly deformed chelate rings of complex **12** are shaded.

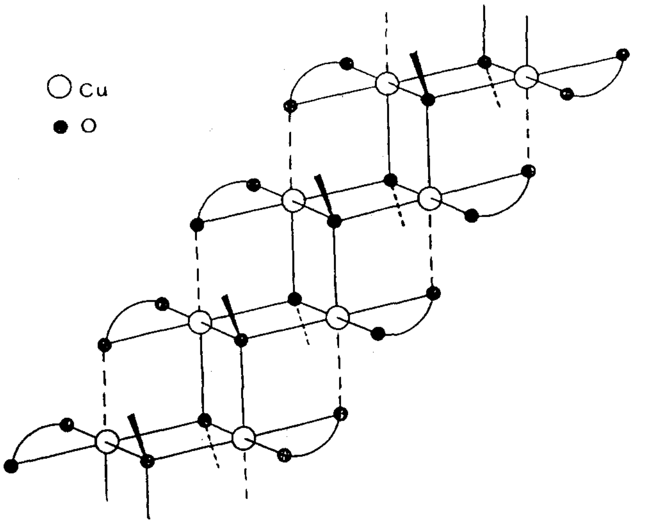

Figure 6. Hypothetical structure of the double-chained polymer ladder Cu, O structure on the basis of the inner Cu, O framework of the complex **12** as an elementary unit. The Cu atoms have the same 4 + 1 + 1 hexacoordination as Cu(1) atoms and μ_3-bridged O atoms as O(6) atoms in **12**.

only one possible stacking arrangement of dimeric Cu units. The necessary rotation of dimers with a concomitant displacement along the long axis of the polymer (perpendicular orientation of the long axes of neighboring dimeric units observed in **6** or **14**) does minimize steric repulsions between the bidentate ligands. A systematic analysis of potential polytypic polymer structures was performed[19] for the stacking of pseudoplanar oligomers $Cu_nX_{2n}L_2$ ($X = Cl^-$, Br^-, Cl^-, Br^- or a neutral ligand) using a spin-Hamiltonian approach to predict the possible stacking patterns. The proposed ladderlike structure corresponds to one (phase 1,1,1,1) of four polytypes obtained for nearest-neighbor stacking patterns, all of which were observed experimentally.[19]

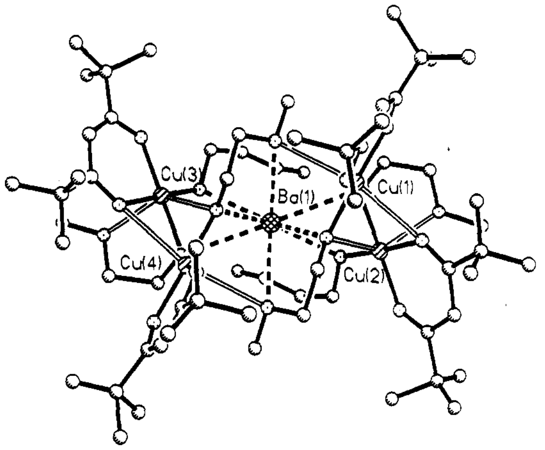

Figure 7. Structure of complex **15**. The additional Cu···O interactions are shown by open lines, and the Ba···O interactions are shown by dotted lines.

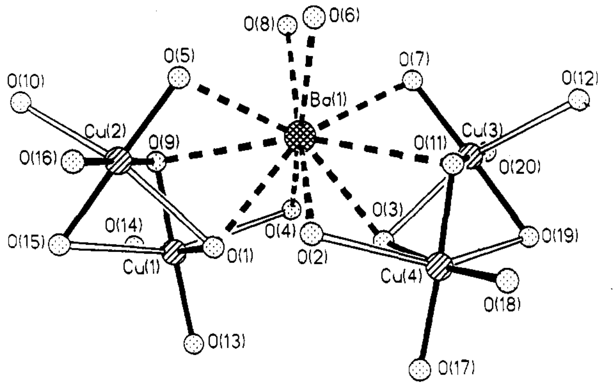

Figure 8. Cu, Ba, O framework of complex **15**.

Complex $BaCu_4C_{62}H_{118}O_{20}$ (15). The structure of the complex **15**, which has approximate C_2 symmetry (Figures 7 and 8), may be viewed as consisting of two binuclear units. They are connected by a Ba^{2+} cation. The contact within these binuclear building blocks is considerably weakened by the Ba···O interactions. The presence of two bicopper units in **15** seems to be essential, because in **12** they have been identified as the inner tight core. The Ba^{2+} cation coordination is completed by the O atoms of two additional 2-methoxyethoxide ligands. All Cu atoms in **15** acquire a distorted octahedral geometry. The binding of O_{acac} atoms in a μ-position with the weaker interactions Cu(1)···O(15) = 2.70 (2) Å, Cu(2)···O(1) = 2.44 (2) Å, Cu(3)···O(3) = 2.45 (2) Å, and Cu(4)···O(19) = 2.73 (2) Å is quite unusual and up to now observed only in ladder tetranuclear species like **12**.

Another unusual feature of **15** is the existence of three oxygen bridges between the Cu atoms within each of the couples Cu(1), Cu(2) and Cu(3), Cu(4), one symmetrical (O(9) for Cu(1), Cu(2); O(11) for Cu(3), Cu(4)) and two nonsymmetrical of the Cu–O···Cu type. The additional axial Cu···O interactions on the Cu(1) and Cu(4) atoms are remarkably weaker (Cu(1)···O(4) = 2.82 (2) Å, Cu(1)···O(15) = 2.70 (2) Å, Cu(4)···O(2) = 2.80 (2) Å, Cu(4)···O(19) = 2.73 (2) Å) than for the Cu(2) and Cu(3) atoms (Cu(2)···O(1) = 2.44 (2) Å, Cu(2)···O(10) = 2.55 (2) Å, Cu(3)···O(3) = 2.45 (2) Å, Cu(3)···O(12) = 2.53 (2) Å). The approximate symmetries of these separations are in agreement with the very small deviations of the Cu atoms from the corresponding basal planes (0.013, 0.008, 0.009, and 0.003 Å for Cu(1), Cu(2), Cu(3), and Cu(4), respectively).

Two closed Cu_2BaO_4 moieties (Cu(1)Cu(2)BaO(1)O(4)O(5)O(9)O(4) and Cu(3)Cu(4)BaO(2)O(3)O(7)O(11)) can be distinguished within the Cu, Ba, O framework of **15**. The large

---

[19] Willett, R. D.; Bond, M. R.; Pon, G. *Inorg. Chem.* **1990**, *29*, 4160.

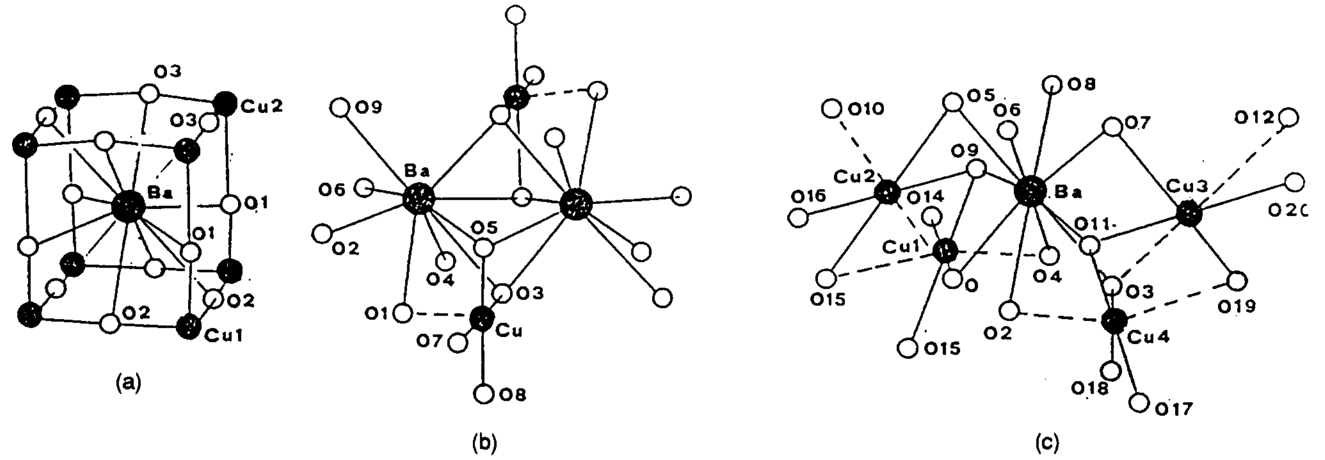

Figure 9. Ba atom coordination in the perovskite type unit of the structure $YBa_2Cu_3O_7$: **19** (a); **18**[20] (b); **15** (c). The additional Cu···O interactions in **15** and **18** are shown by dotted lines.

deviation from linearity of the axial O···Cu···O fragments (154.1 (7), 138.6 (7), and 138.5 (7)° for Cu(1), Cu(2), Cu(3), and Cu(4), respectively) can be ascribed to the geometrical constrains due to the closeness of these Cu_2BaO_4 moieties.

The Ba atom is 10-coordinate. The Ba–O distances range from 2.676 to 3.019 (17) Å, which is a normal phenomenon in Ba coordination chemistry, e.g. 2.668–2.982 (4) Å in the complex $Ba_2Cu_2(acac)_4(OCH_2CH_2OCH_3)_4{\cdot}2HOCH_2CH_2OCH_3$ (**18**).[20] The coordination polyhedron of Ba in **15** can be described as a trigonal prism with four capping atoms (O(2), O(4), O(6), O(8)). The Ba–O interactions with the capping O atoms (2.883–3.019 (17) Å) are essentially weaker than with the O atoms at the vertices of the trigonal prism (2.676–2.768 (17) Å), which on the one hand emphasizes the closeness of the mentioned Cu_2BaO_4 moieties and on the other hand indicates a potential break up of **15** in the directions of the Ba···O(capped) interactions.

The question on the structural relationship of mixed Ba, Cu complexes to the $YBa_2Cu_3O_7$ phase (**19**) is of special interest. The Ba polyhedra in the structures **19**, **18**, and **15** are oriented such that they allow a comparison in the schematic Figure 9. One can see that the positions of two Cu atoms of **18** correspond to the positions of the Cu1 and Cu2 atoms in **19**. The orientations of the vectors of some Ba–O bonds also coincide in both structures. The smaller coordination number of the Ba atom in **18** (nine Ba···O interactions at 2.770–2.977 (8) Å; see e.g. ref 21) can be attributed also to the steric protection by the surrounding bulky ligand.

The difference of the mutual arrangement of Ba and Cu in the structures **19** and **15** is easier to understand from a comparison of the metal···metal separations. The Ba···Cu distances in **15** are only somewhat larger (3.668, 3.525, 3.529, and 3.675 (4) Å for Cu(1), Cu(2), Cu(3), and Cu(4), respectively), while the closest Cu(1)···Cu(2) and Cu(3)···Cu(4) contacts of 2.999 and 3.002 (4) Å are typical for dimeric Cu complexes and are much less than Cu···Cu distances of 3.8640 (4) Å in **19**.[21] The Cu···Cu distances of 5.605–7.003 (4) Å between the related by pseudo-2-fold axis of the $BaCu_2O_4$ moieties in **15** are much greater than the closest Cu···Cu separation in **19**. Thus, the projection of the coordinative environment of the Ba and Cu atoms in the framework of **15** into **19** requires only minor structural distortions, an increase of Cu(1)···Cu(2) and Cu(3)···Cu(4) distances with simultaneous decrease of separations Cu(1)···Cu(4) and Cu(2)···Cu(3). Thus, the structure of **15** may be viewed in first approximation as one possibility of a structural deformation of **19**, e.g. via increase of the coordination number of metal atoms.

To uniformly describe the inorganic cores of **15** and **18**, a simple way[22] was used for the representation of the M, Cu, O cores of a given stoichiometry in terms of small building blocks which are related to the perovskite unit. With application of mapping of building blocks, the crystal structure of the given inorganic crystal can be established; e.g., joining of two $CuBaO_n$ blocks carrying the charge $q = 0$ or -1 when $n = 2.0$ or 2.5 with the $CuLnO_2$ block ($q = +1$) generates the $LnBa_2Cu_3O_x$ structure. For the construction of the core of **15** the Cu(2) and Cu(3) atoms have to be artificially shifted along the diagonals of the corresponding parallel faces. By this rough approximation only the Ba atom surroundings in **15** and **18** can be generated. The cores of the structures **15** and **18** do not resemble the "infinite" CuO_2 planes and cannot be considered as secondary blocks[22] with the composition $Cu_{0.25}BaO_{2.25}$ (**18**) and $Cu_{1.25}BaO_{2.5}$ (**15**). The calculation of the formal charge of the building blocks in the case of definite molecular compounds is not quite as straightforward as in the case of inorganic structures with a simple and clear periodicity. Apparently the building block model can be successfully applied by taking molecular structures **15**, **18**, and other related complexes, which seems to be useful in the elucidation of models of structural transformation of molecular complexes to the desired oxide structures.

As one can see from the Figures 1–4 and 7 and Tables II–VI the terminal *t*-Bu and especially CF_3 groups exhibit increased thermal movement, viz. rotation around the exocyclic C–C bonds. Nevertheless, there is no disordering of these groups, which is quite usual for the Cu complexes with a CF_3 group environment (see e.g. ref 23). At the same time, contacts of the CF_3 groups constitute the majority of shortest intermolecular distances in the crystals (see also the discussion of CF_3-surrounded Li clusters[24]). But all the contacts of the CF_3 groups exceed the corresponding sum of Van der Waals radii. The largest repulsive contribution of the atoms of the CF_3 groups was observed in the crystal of the complex $Cu(C_{10}H_6F_3O_2)_2$,[25] for which a calculation by the atom–atom potential method was performed. So, the presence of *t*-Bu and especially CF_3 groups promotes the weakness of intermolecular interactions and therefore obviously enhances the volatility of Cu complexes.

Conclusion

The presence of bulky pentafluorophenyl substituents at the bridging oxygen atoms in the dimeric square-planar complex **10**

---

(20) Sauer, N. N.; Garcia, E.; Salazar, K. V.; Ryan, R. R.; Martin, J. A. *J. Am. Chem. Soc.* **1990**, *112*, 1524.

(21) Nakai, I.; Sueno, S.; Okamura, F. P.; Ono, A. *Jpn. J. Appl. Phys.* **1987**, 788.

(22) Nardin, G.; Randaccio, L.; Zangrando, E. *Acta Crystallogr.* **1989**, *B45*, 521.

(23) Angren, M.; Turpeinen, U.; Hämäläinen, R. *Acta Crystallogr.* **1982**, *B38*, 429.

(24) Bidell, W.; Shklover, V.; Berke, H. *Main Group Met. Chem.* **1991**, *14*, 137.

(25) Baidina, I. A.; Stabnikov, P. A.; Igumenov, I. K.; Borisov, S. V. *Koord. Khim.* (in Russian) **1986**, *12*, 543.

does provoke the coordination of THF molecules in the fifth coordination site of the Cu atoms with formation of basal-edged pyramidal geometry. This on the other hand prevents coordination of the sixth site and/or subsequent association into tetramers. The series of shortened intramolecular noncovalent contacts enforces a large rotation of the C_6F_5 ring (67.1°) relative to the Cu_2O_2 moiety, which explains the absence of significant anomalies in Cu···Cu and Cu–O interactions under the influence of these σ-acceptor substituents.

The outer Cu···O(THF) interactions in the cubanelike tetramer **6** are somewhat stronger, while the corresponding intracore interactions are slightly weaker than in the cubane-like tetramer **14**, where the intramolecular character of Cu···O interactions leads to some larger distortion of the coordination geometry around the Cu atoms. The partial rehybridization of bridged O atoms on formation of tetranuclear **6** and **14** leads to a tetrahedral distortion of the equatorial surroundings of the Cu atoms and can be even envisaged as a way to release strain caused by intramolecular steric overcrowding.

The parallel orientation of the long axes of the approaching Cu, O dimers leads to formation of a tetranuclear ladderlike oligomer **12** which shows different interdimer Cu···O separations in contrast to equal ones in the cubane-type structures **6** and **14**. The nearly perpendicular orientation of the neighboring four-membered Cu, O moieties in the framework of **12** corresponds to mutually perpendicular direction of bonds at neighboring Cu atoms which led us to propose the existence of a polymeric double-chain Cu, O structure with an identity period of 3.37 Å, viewing **12** as a simple oligomeric precursor.

The use of a simple pictorial approach allows the description of the Ba, Cu, O framework **15** in relation to the Ba, Cu, O complex **18** and the perovskite structure **19**, via composition of elementary Ba-centered building blocks ($Cu_{1.25}BaO_{2.5}$, $Cu_{0.25}BaO_{2.25}$, and $CuBaO_2$ or $CuBaO_{2.5}$, respectively).

The present structural investigation, attempted via a closer study of even simple molecular complexes and interrelations with solid-state compounds, gives insight into structure-dependent properties of oxides, e.g. phase changes, variation of oxygen content, or possible variation of coordination environment to the metal atoms.

Acknowledgment. We are indebted to Dr. H. Schmalle for the collection of intensities for crystal **14** and to H.-U. Hund for participation in the structure determinations of compounds **14** and **15**. We thank the Swiss National Science Foundation for financial support.

Supplementary Material Available: Tables S1, S5, S9, S13, and S17, listing anisotropic displacement parameters, Tables S2, S6, S10, and S14, listing H atom coordinates, Tables S3, S7, S11, S15, and S18, listing bond lengths, and Tables S4, S8, S12, and S16, listing bond angles, and Figures S1–S6, showing atom numbering in the complexes (29 pages). Ordering information is given on any current masthead page.